TU Delft

Delft University of Technology

Densor: An Intraoral Battery-Free Sensing Platform

Dsouza, V.K.P.; Pronk, J.S.; Peppelman, C.A.; Madariaga, Víctor Ignacio ; Pereira-Cenci, Tatiana; Loomans, Bas ; Pawełczak, Przemysław

DOI
10.1145/3699746

Publication date
2024

Document Version
Final published version

Published in
ACM Proceedings on Interactive, Mobile, Wearable and Ubiquitous Technologies

Citation (APA)
Dsouza, V. K. P., Pronk, J. S., Peppelman, C. A., Madariaga, V. I., Pereira-Cenci, T., Loomans, B., & Pawełczak, P. (2024). Densor: An Intraoral Battery-Free Sensing Platform. *ACM Proceedings on Interactive, Mobile, Wearable and Ubiquitous Technologies*, *8*(4), Article 191. https://doi.org/10.1145/3699746

Important note
To cite this publication, please use the final published version (if applicable).
Please check the document version above.

Copyright
Other than for strictly personal use, it is not permitted to download, forward or distribute the text or part of it, without the consent of the author(s) and/or copyright holder(s), unless the work is under an open content license such as Creative Commons.

Takedown policy
Please contact us and provide details if you believe this document breaches copyrights.
We will remove access to the work immediately and investigate your claim.

This work is downloaded from Delft University of Technology.
For technical reasons the number of authors shown on this cover page is limited to a maximum of 10.

Densor: An Intraoral Battery-Free Sensing Platform

VIVIAN DSOUZA, Delft University of Technology, The Netherlands
JEFFREY PRONK, Delft University of Technology, The Netherlands
CHRISTIAN PEPPELMAN, Delft University of Technology, The Netherlands
VÍCTOR IGNACIO MADARIAGA, Radboud University Medical Center, The Netherlands
TATIANA PEREIRA-CENCI, Radboud University Medical Center, The Netherlands
BAS LOOMANS, Radboud University Medical Center, The Netherlands
PRZEMYSŁAW PAWEŁCZAK, Delft University of Technology, The Netherlands

The mouth offers valuable insights into the condition of the human body. Yet, deploying intraoral sensors to measure oral temperature or jaw movements poses challenges in safety and acceptability. Consequently, real-world data for intraoral research is scarce. To address this gap, we leverage the widespread use of dental retainers and enhance them with Densor: an electronic sensing platform requiring only a standard smartphone for charging and data retrieval using a Near Field Communication interface. Its low power architecture enables prolonged sensing on a single charge, making it suitable for sleep studies. It can provide practitioners with feedback on treatment compliance, and is even able to detect if the user is speaking or drinking water. Densor presents an intraoral, actively powered, battery-free platform featuring multi-modal sensors and an extended lifespan.

CCS Concepts: • **Computer systems organization** → *Embedded systems*; **Sensor networks**.

Additional Key Words and Phrases: Intraoral sensor, Battery-free systems

ACM Reference Format:
Vivian Dsouza, Jeffrey Pronk, Christian Peppelman, Víctor Ignacio Madariaga, Tatiana Pereira-Cenci, Bas Loomans, and Przemysław Pawełczak. 2024. Densor: An Intraoral Battery-Free Sensing Platform. *Proc. ACM Interact. Mob. Wearable Ubiquitous Technol.* 8, 4, Article 191 (December 2024), 30 pages. https://doi.org/10.1145/3699746

1 Introduction

Head-worn platforms—smart glasses [19] and smart earpieces (earables) [63, 107] being the principal ones—allow for continuous monitoring of signals correlated with the state of the human body. Unfortunately, neither smart glasses nor earables allow sensing from within the mouth.

Measuring directly inside the human mouth is beneficial, as the oral cavity is a source of unique signals that are very hard to measure (like tongue movement [62]) or even impossible to measure (like biological markers [77]) with sensors worn outside the mouth. Unfortunately, as there are no widespread intraoral sensors available, many clinical applications, such as dental care, still rely on subjects being tested with dedicated tools in a medical

Authors' Contact Information: Vivian Dsouza, Delft University of Technology, Delft, The Netherlands, v.k.p.dsouza@tudelft.nl; Jeffrey Pronk, Delft University of Technology, Delft, The Netherlands, j.s.pronk@student.tudelft.nl; Christian Peppelman, Delft University of Technology, Delft, The Netherlands, peppelmanc@gmail.com; Víctor Ignacio Madariaga, Radboud University Medical Center, Nijmegen, The Netherlands, victor.madariagarivera@radboudumc.nl; Tatiana Pereira-Cenci, Radboud University Medical Center, Nijmegen, The Netherlands, tatiana.pereira-cenci@radboudumc.nl; Bas Loomans, Radboud University Medical Center, Nijmegen, The Netherlands, bas.loomans@radboudumc.nl; Przemysław Pawełczak, Delft University of Technology, Delft, The Netherlands, p.pawelczak@tudelft.nl.

This work is licensed under a Creative Commons Attribution-ShareAlike 4.0 International License.
© 2024 Copyright held by the owner/author(s).
ACM 2474-9567/2024/12-ART191
https://doi.org/10.1145/3699746

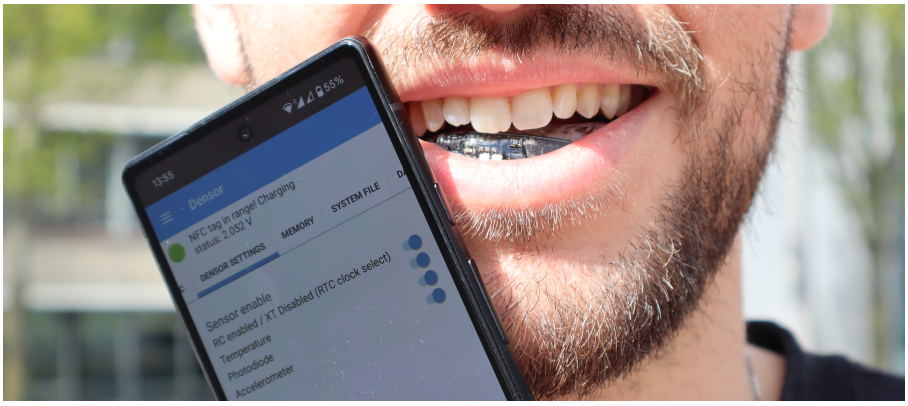

Fig. 1. The developed intraoral battery-free sensing platform. A contemporary NFC-enabled smartphone charges, interacts and collects data from a battery-free sensor embedded in a dental retainer.

professional-assisted setting to collect single point of measurement, without the ability to correlate the test result with data from the subject's day-to-day life.

Naturally, there are continuous efforts in building sensing platforms that allow for long-term and reliable sensing of various signals from the human mouth, as we will discuss extensively in Section 2. Unfortunately, their abilities lag behind other head-worn wearables. Simply put, it is hard to keep intraoral sensors powered continuously, yet miniature and safe to use. Then, many sensors are bulky, making real-life data collection from humans cumbersome. Moreover, most intraoral sensors require specialized equipment to charge and read the data, as we will also discuss in detail in Section 2. We conclude that, due to engineering challenges in deploying intraoral sensors, improvements in understanding oral functions or finding indicators of diseases remain unidentified. To address the above challenges, we present *Densor*[1]—an intraoral battery-free sensing platform. The contributions of this paper are:

Contribution 1: **Design and implementation of a battery-free and actively powered intraoral sensing system.** Unlike other intraoral sensing platforms that rely on (potentially toxic) batteries, the Densor is battery-free—increasing both safety and acceptability. It charges quickly via a Near Field Communication (NFC) interface (while being fully enclosed in a dental aligner), and stores the energy to actively perform measurements, even in the absence of an external reader.

Contribution 2: **Long lifespan sensing system that is both small and easy to use and fabricate.** Densor's ultra low power architecture enables a prolonged lifetime (for example: 7 h with a sample every 2 min), due to the power consumption at idle time not exceeding 72 nW (22 nA at 3.3 V supply). It is space-optimized—allowing it to be embedded seamlessly in a standard orthodontic plastic aligner. Fabrication of the device does not require any specialized equipment that would not be already available to a dental technician. Operating the device requires only a smartphone, and its antenna design enables use without removal from the mouth.

Contribution 3: **Multi-modal, expandable framework introducing novel sensing methodology.** Densor introduces multi-modal intraoral sensing from jaw position, oral temperature and mouth opening state simultaneously. We detect mouth opening by measuring the amount of light entering the mouth.

[1]A portmanteau of a word 'dental' and 'sensor'.

Densor's design, including all datasets and code accompanying this publication, will be released to the public domain [1]. This will allow other research groups to build Densor themselves, democratizing intraoral sensing, which so far has been accessible to only a small set of research laboratories.[2]

2 Intraoral Sensing: Background and State of the Art

Sensing and transmitting data from a human mouth is a captivating concept. As we show in this section, it is still not fully resolved, and sometimes leads the media to spread hoaxes around what is possible with tooth-based transmission and sensing [132]. Nonetheless, the concept of developing specialized sensors for monitoring signals inside the human mouth dates back to at least 1966, when a sensor was designed to measure intraoral fluoride concentration [53, 54]. However, fluoride is just one example of various modalities that can already be measured from within the mouth.

2.1 Uniqueness of Intraoral Sensing

Intraoral sensors offer unique measurement capabilities not achievable with other on-body sensors. We summarize all the various applications of intraoral sensing[3].

Sensors that monitor jaw movements provide insight into eating and speaking habits, as well as pointing to certain physiological conditions such as (sleep and awake) bruxism (grinding or clenching teeth). Efforts to detect and mitigate bruxism using intraoral sensors have been both academic [94], and commercial [25, 26, 86, 113]. Studies have also used jaw movements to monitor diet based on chewing patterns [33].

The oral cavity is also an ideal location to install an accelerometer for measuring head concussion in impact-heavy sports (such as American football), where the use of other head-worn sensors is undesirable [49, 50].

Saliva is a source of many biomarkers which can be measured by an intraoral sensor [12, Table 2]. Many systems measure in vivo saliva-based biomarkers such as pathogenic bacteria [82], lactic acid [69], uric acid [67], sodium [76], or glucose [9]. Some studies harvest energy wirelessly using NFC for instantaneous use to monitor fluoride levels for drug delivery [114].[4] Development of intraoral sensors to measure such biomarkers is a topic of current interest [89].

The oral temperature can serve as an indicator of a disease, and also monitor its progression. Therefore many studies use intraoral sensors to measure temperature inside the human mouth [47, 70, 96]. Dentistry-related intraoral sensing applications include intraoral pressure sensing [72], bite pressure sensing [32], tooth occlusion [57, 95], prostheses monitoring [109], or orthodontics retainer monitoring [52]. Another application of intraoral sensing is the wireless control of remote objects. Such systems reside on the intersection of epidermal and pass-through technologies for human computer interaction [90, Figure 3]). Applications include assistive technology for people with disabilities [98] (see also Table 1, second column) and silent wireless control [28]. We speculate that tongue position and tongue thrusting are other oral-based signals that can be measured with much better accuracy by intraoral sensors instead of external sensors [84].

[2]It will also expose the mobile and ubiquitous systems community to the intraoral sensing, which so far has been largely constrained to the application of tooth brushing monitoring [5, 31, 58, 135].

[3]For the in-depth exposure to intraoral sensing we refer the reader to recent survey papers [37, 77]; see also [14, Section "Saliva-Based Sensors"].

[4]To the best of our knowledge, in vivo monitoring of oral moisture (another biomarker indicating dehydration or xerostemia [dry mouth syndrome]) has not been demonstrated, as state of the art measurement rely on out-of-mouth sensors [48].

Table 1. Comparison of intraoral sensing platforms classes, grouped per wireless interface, except for the last column representing commercial realization of an intraoral sensor. Colour code: denotes undesired feature and denotes the desired feature.

	This work	[98][1]	[49, 50][2]	[76][3]	[47]	[52]	[114][4]	[71, 86][5]
Study type	Sleep	Teleoperation	Concussion	Sodium	pH	Retainer use	pH	Retainer use
Dimension x [cm]	4.6‡	3.5	⊖	2.1	1.6	1.3 (radius)	1.0	1.2
Dimension y [cm]	8.0‡	2.5	⊖	2.7	1.05	⊖	0.8	0.8
Dimension z [cm]	0.9‡	⊖	⊖	0.2	0.08	⊖	0.15	0.45
Total weight	0.26 g‡	75 g	⊖	1.5 g†	⊖	⊖	0.09 g	0.4 g
Power use	0.11 mW◇	3.7 mW	⊖	⊖	⊖	3 µW*	⊖	⊖
Wireless interface	NFC	DBC	⊖	BLE	ANT	RFID	NFC	RFID
Sampling rate	<1 Hz	64 Hz	<5.5 kHz	⊖	0.5 Hz	<1/600 Hz	N/A	<1/900 Hz
Sensors	𝔸, 𝕃, 𝕋	𝕄	𝔸	𝕊	ℙ, 𝕋	𝕋	ℙ	𝕋
Attachment	LJA	HPR	LJA	HPR	VFS	HPR	TWS	OOA
Data reader	SP	CM	⊖	SP	SP	RD	SP	CM
Battery-free	Yes	No	No	No	No	No	Yes	No
Reader-free sensing	Yes	Yes	Yes	Yes	Yes	Yes	No	Yes
Open source	Yes	No	No	No	No	No	No	No
Harvesting energy	Yes	No	No	No	No	No	Yes	No

Symbols: ⊖ (unspecified); **Wireless interface**: ANT+ (ANT), Bluetooth Low Energy (BLE), 27/432 MHz OOK/FSK (DBC), 13.56 MHz NFC (NFC), ISO-IEC 14443 RFID (RFID); **Sensor types**: Accelerometer (𝔸), light (𝕃), magnetic (𝕄), sodium (𝕊), pH (ℙ), temperature (𝕋); **Attachments**: HPR (Hawley palatal retainer), LJA (lower jaw aligner), OOA (on-aligner attachment), TWS (teeth whitening strips) VFS (vacuum-formed [palatal] splint); **Readers**: smartphone (SP), RFID reader (RD), custom reader (CM)
‡ w/o aligner/retainer † with battery * at idle ◇ with a sampling rate of 1 Hz, which was the highest sampling frequency our app (Section 6.2.2) can support (note: power consumption reduces with larger sampling interval)
[1] Similar platforms: [73] (transmitter circuit only), [30, 97] [2] Related work: [29, 78]; Similar platforms: [43], [16] (battery outside mouth), [105] [3] Similar platforms [8, 10] (glucose measurement), [94] (bruxism detection), [33] (food intake), [85] (tongue pressure measurement), [68] (uric adic detection) [4] Related work: [82, 128] [5] Other commercial platforms: [13] (teleoperation), [80] (pH level), [3, 25, 26, 86, 113] (bruxism), [23] (retainer use)

2.2 State of the Art in Autonomous Intraoral Sensing Platforms

A summary of all relevant platforms presented in recent years is given in Table 1. To the best of our knowledge, this is the most comprehensive summary of all autonomous[5] intraoral sensing systems, which are demonstrated by in vivo experiments with human subjects.

We observe that there are already plenty of existing intraoral sensing platforms built around popular low-power communication protocols. Moreover, the set of commercial intraoral sensing platforms is also growing (see last column of Table 1). On the other hand, all platforms are either battery-based or passive systems. Not only are batteries less acceptable for wearing in-mouth (see Section 7.3.3), but also recharging them is hard [47, 76]. Some systems have non-replaceable batteries [52], or a protruded battery on a dental brace causing wear discomfort in the long term [49, 50]. Platforms that allow harvesting ambient energy to power the intraoral system are passive and only work in the presence of an external reader [114]. Function-wise, all summarized works measure up to two sensing modalities. Some of them are large and bulky [98], or require dedicated (non-smartphone based) readers and chargers.

We conclude that the work on a functional intraoral sensor is far from over—not only because of the technical challenges of size, energy provision and convenience of use, but also from the unexplored domain of signals originating from the mouth.

[5]Autonomous in the sense of being fully embedded in the mouth without cabled attachments to external devices.

3 The Oral Cavity: A Potent Signal Source for Body State Inference

Beyond biological research, the intraoral cavity is a source of signals that have a much better signal quality than measurements from traditional on-body sensors. While Densor has many potential applications, we focus on the sleep-study related measurements—a core application for intraoral sensors.

3.1 Mouth Opening State

Determining the state of mouth opening while asleep is a powerful diagnostic tool in sleep quality studies [66]. Importantly, sleeping with the mouth open is deemed to be a risk for Obstructive Sleep Apnea (OSA)—a disorder where the upper airway is partially or completely obstructed during sleep [66]. At present, OSA studies rely on video [134] or external transducers attached to the face [129] to determine the mouth position. We postulate that these methods are unappealing and cumbersome. Reasons being—participants have to be recorded (breaching privacy) or wear extra external sensors attached to the head that can detach while sleeping. To overcome this limitation, an Inertial Measurement Unit (IMU) can be embedded in the aligners worn by the patients for treating sleep disorders (examples include [102, 117]), to collect data about the mouth opening state, and monitoring the status of treatment in parallel.

3.2 Head Position During Sleep

The severity of OSA also depends on the position of the head while asleep. By measuring the head position using intraoral sensors, practitioners of positional therapy can receive feedback on the effectiveness of efforts in mitigating the severity of OSA [116]. Sleep posture data helps preventing bedsores in post-surgery recovery, and in warning patients suffering from epilepsy [136]. Monitoring the head position during sleep may also be important for studies measuring tooth decay, as saliva accumulates on the side one sleeps on. This information could also be indicative of overall sleep quality, and may help diagnose causes of body aches and sores after sleep.

Prior studies have measured body posture during sleep using on-body sensors [56], or even non contact methods using radio frequency [136] or vision [116]. However, all of these methods require either dedicated hardware, i.e. external signal sources, or the user to wear an extra device to sleep. We posit that since many people already wear aligners for orthodontic treatment to sleep—they can be repurposed with additional electronics such as an accelerometer to measure these signals without additional discomfort. We can infer the position of the head during sleep by obtaining the roll and pitch angle from the raw values of the accelerometer [119, Equation 6 and 7]. This can be done even with sparse sampling as only a single measurement is required to infer the head orientation.

3.3 Jaw Movement Classification

There is a large body of work on the inference of jaw movements from wearables, such as ear-worn sensors. These ear-worn devices use various sensors for jaw movement detection, such as microphones [6], barometers [7], IMUs [20], or proximity sensors [18].[6] Other methods include sensing reflections of smartphone-induced audio signals projected to the ear canal [27]. However, head-, or ear-worn sensors in particular, have two main limitations: (i) they can have negative health consequences when worn during sleep (like wax buildup and bacterial infections) [34], and (ii) they are positioned away from the jaw which causes low measurement precision.

3.4 Sensor Fusion

The ability to measure all of these parameters simultaneously allows us to understand their relations, which itself provides new insights. By time synchronising them to other external sources (such as heart rate and audio

[6]For in-depth discussion on these and other techniques of jaw (and tongue) movement detection see [27, Sec. II].

recordings), they can also be fused to offer a deeper understanding of sleep quality. The multi-modal input also helps simplify activity detection as signals from some sensors can be used to activate other sensors.

4 Intraoral Sensor Requirements

Based on the current state-of-the-art outlined in Table 1 and potential capabilities of intraoral sensors, we identify the following set of requirements that must be met by intraoral sensors.

Requirement ❶: **Contactless transmission.** To protect the user from contact with the electronics and mitigating the risk of electrical shock, the system must be completely sealed. This necessitates a contactless transmission interface for interaction. The **key challenge** is that wireless transmission techniques require some space on the Printed Circuit Board (PCB) for energy storage and an antenna, while the space in the mouth is very limited.

Requirement ❷: **Energy harvesting-based.** For user convenience, an ideal intraoral sensor should utilize energy harvesting for power. While prior studies have used NFC for energy harvesting, they do not store the energy for later use. The **key challenge** is to sustain continuous operation without the presence of an external charger.

Requirement ❸: **Battery-free.** Toxic elements in batteries limit their suitability for intraoral sensing. The **key challenge** is that although (super-)capacitors allow for fast charging, they have much lower energy density than batteries, which results in shorter operation times.

Requirement ❹: **Long life.** Battery-free requirements necessitate an ultra-low power processing and communication architecture. Further, many signals from intraoral sensors are either transient or continuously changing, requiring continuous sampling. Because of this, the device must be able to collect periodic samples over a significant enough period (for example: a full night's sleep) to draw meaningful conclusions. The **key challenge** is that even low power sensors drain small capacitors within hours (or even minutes) when powered continuously.

Requirement ❺: **Free of dedicated external hardware.** The challenge with small and complex low-power systems is that they are often difficult to use. In order to improve the adoption of intraoral devices, they should be easy to use without reliance on external hardware or expertise. The **key challenge** is to harvest and store energy, as well as communicate with the system using no more than a commodity, NFC-enabled smartphone.

Requirement ❻: **Acceptable to wear.** Intraoral sensors must be worn on teeth without obstructing normal oral function, ensuring suitability for daily use. We do not expect sensor sizes to become small enough to make them nearly invisible in the near future. The **key challenge** is that the intraoral sensor should be lightweight and fit in a regular dental aligner (not larger than 11.57 mm in height[7] and 10.8 cm in length, measured between left and right second molar [111, Table 1-7]).

Requirement ❼: **Extendable and open source.** Many people worldwide have undergone orthodontic treatment involving on-tooth devices such as aligners and retainers. This indicates a significant potential for intraoral sensors and oral data collection for research purposes.[8] Intraoral sensing platforms should be available under an open source license, enabling the democratisation of intraoral sensing. Further, expanding the platform with new sensors should be easy. The **key challenge** is that new solutions for intraoral sensing have to be developed from scratch. The mobile systems community needs an equivalent for intraoral sensing, as OpenEarable [107] and eSense [63] are for ear-centered sensing.

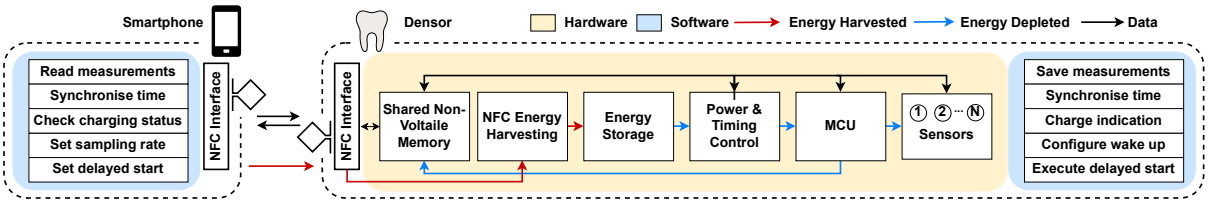

Fig. 2. Densor system architecture showing the interaction between the user and system via the smartphone app.

5 Densor Architecture

Addressing the above requirements we propose Densor: a new system architecture for intraoral sensing presented in Figure 2. Each component of Densor is described below.

5.1 Hardware

5.1.1 Communication and Data Storage. Requirement ❶ and ❺, entail the use of a wireless interface that is compatible with most modern smartphones. We believe that as sleep-related data can be downloaded after waking up, continuous active transmission is unnecessary. Thus, similar to previous studies [114], we propose using an NFC interface and also using the on-board Non-Volatile Memory (NVM) of the tag to store measurements. The tag should be NFC Forum-compatible [93] (i.e. ISO/IEC 15693 [61] and in particular ISO/IEC 14443 [60] standard for short, centimeter range, distances) and operate at the 13.56 MHz base frequency.

5.1.2 Energy Harvesting. To address Requirement ❷, we need a reliable source to harvest and store energy. Existing intraoral platforms that harvest energy from NFC do not store it for later use, preventing both the sensor's continuous operation and reader-independent data collection. Alternatively, studies also harvest energy from bite [41, 59] and mastication [15]. Thermal energy could be harvested from the temperature gradient between the body and the environment (such as consumed liquids).[9] When evaluated experimentally (see Appendix B), we found that the thermal energy harvested is insufficient to power Densor continuously. Instead, similar to prior studies [114, 137], we harvest energy from the NFC interface used for communication as this is the most reliable energy source.

5.1.3 Energy Storage. To meet the needs of Requirement ❸, we propose to use capacitors in place of batteries. This architecture adds Densor to the set of similar battery-free systems [38, 51, 133].

5.1.4 Power and Timing Control. Addressing requirement ❹ is challenging. Despite using low-power sensors, energy would be drained from the storage capacitor(s) rapidly if Densor is kept continuously powered. As the harvested energy stored on the capacitors is limited, it is imperative that we save and expend this power carefully. To overcome this, we use a low power Real-Time Clock (RTC) with power switch for power management, following the architecture presented by Kazdaridis et al. [64], which is used in similar low power systems [133, Sec. 4.1], [39]. This means that the Microcontroller Unit (MCU) and sensors are completely powered off in the inter-sample period, with only the RTC powered to determine wake up time. This method achieves better power saving than deep-sleep or any of the low power run modes of the MCU.

[7] Estimated as the average height of the second molar of 7.7 mm [111, Table 1-7] plus the smallest vestibular depth of 3.87 mm in the mandible measured at the youngest (6–14 years) group age [91].
[8] In the US, between 1989 and 1994 about 50% of 12-17 year olds were reported to have received orthodontic treatment [101, Fig 1.21].
[9] Thermal harvesting was used to power non-intraoral embedded sensing platforms, such as [17].

5.1.5 Computation and Sensing. In this work, we include three sensing modalities: (i) position, (ii) light and (iii) temperature. For position measurement we exploit a low power three-axis accelerometer, as it is suitable to measure head position during sleep with sparse sampling, following the insight presented in Section 3.3. For light measurement from the oral cavity we apply a photodiode, as per the insight presented in Section 3.1. Finally, for oral temperature measurement we include a temperature sensor, as explained in Section 3.4. To interface with these sensors and save measurements, we advocate using the most powerful processor that meets our size (Requirement ❻) and power constraints (Requirement ❹). This enables us to keep our system ready for future expansion as per Requirement ❼.

5.2 Software Stack

5.2.1 User Control. To satisfy Requirement ❺, the user must be able to interact and charge the Densor using only a smartphone. The smartphone app should implement a set of features that makes the Densor configurable and user-friendly. The following features are implemented as part of the user control.

Data Readout and Densor Reconfiguration. In our architecture, the smartphone interacts with the Densor by using the NFC interface to read the collected data, and write to the configuration registers in the shared memory on the Densor's NFC tag. All these operations are possible without the intervention of the MCU.

Time Synchronisation. In wearable systems, it is crucial to know the time at which specific events were captured. However, as the Densor is intermittently-powered, the MCU cannot sustain a constant clock source. To address this issue, we use the app to synchronise the wall clock time to the Densor. This timestamp is used as a reference with which a timestamp of all subsequent measurements can be determined by counting the elapsed sampling intervals. Moreover, in Densor's architecture, the timestamp is the trigger to start running the measurement process—thus ensuring that all measurements begin from the initial timestamp.

Capacitor Bank Charging Status. As the smartphone is used for charging the Densor capacitors, it is important that the user receives feedback of the capacitors charging status. However, this is challenging because we do not wish to add any circuity to monitor the charging status as this results in a larger power consumption. Instead, we use the MCU to estimate the capacitor voltage by reading its internal voltage reference. This voltage reference can then be used to calculate the supply voltage of the MCU, which is approximately the charge level of the capacitors according to [118]. This calculated supply voltage can then be stored on the NFC tag, which can be read by the smartphone and displayed on the app.

Sampling Rate Control. As Densor is meant to collect data intermittently, the frequency of sample collections has an effect on the total operation time. Therefore, in our architecture, the user can use the app to set the sampling interval as desired.

Delayed Start. Some applications require that a frequent sampling occurs at a later time than when the system was started. For example, a user might want to collect jaw movements in the middle of the night while asleep. Therefore, we provide the ability to begin measurements after an offset period has elapsed. This offset can be set by the user through the app.

5.2.2 Densor Firmware. The Densor adopts a wake-measure-sleep cycle which is controlled by the RTC. As a consequence, in our architecture the MCU is switched off in the inter-sample period. Each time the MCU is switched on, it reads the settings from the NVM to determine the system state. A state diagram describing the wake-measure-sleep cycle is given in Figure 3.

The Densor firmware maps the user control features (see Section 5.2.1) as follows.

Measurements Saving. As the Densor is turned off in between samples, all measurements must be saved to NVM. Generally speaking, a memory pointer is used to keep track of the last save address that has not been written to, and is incremented each time a measurement is saved.

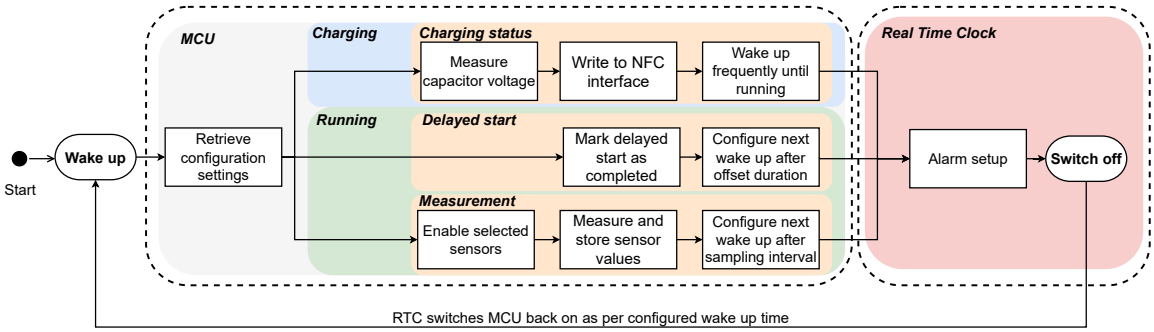

Fig. 3. Densor firmware: state transition diagram.

Time Synchronization. As described in Section 5.2.1, time synchronization on the Densor is enabled by the user writing a timestamp to the Densor's shared memory via the smartphone app. Each time the system wakes up, it checks for the presence of a valid timestamp. If found, it performs a measurement and configures the wake up alarm for the next measurement based on the sampling interval.

Charging Indication. If a timestamp has not been set, it is assumed the user is charging the device. In this case, the MCU calculates the voltage on the capacitors. First an internal voltage reference channel of the Analog to Digital Converter (ADC) is measured. This reference voltage is used to derive the supply voltage as described in [118]. The supply voltage is then stored on the shared memory to be displayed on the app. The MCU then configures the RTC to wake up frequently so that the measurement process can begin shortly after the timestamp is set.

Wake Up Configuration. It is imperative that the MCU must configure the next wake up time correctly. To achieve this, MCU reads the current time from the RTC and increments it by the sampling interval to determine the next wake up time. This calculated value is written to the RTC and the next wake up is enabled, switching the MCU and sensors off until then.

5.3 Densor Intraoral Placement

A significant part of the worldwide population will use dental aligners at some point in their life.[10] Thus, following earlier intraoral sensor designs, we aim at embedding all Densor's electronics into regular orthodontic aligners or retainers. Densor can be attached to both plastic aligners and retainers, as they are made of the same material and differ only in function. Aligners are used during orthodontic treatment to move the teeth into the desired position, while retainers are worn after treatment completion to keep the teeth in position.[11] In consultation with a dentist and a dental technician, we decided to place Densor on the lower jaw, with Densor located on the labial surface (i.e outward facing towards the lips). The choice of labial surface is dictated by two factors: (i) the teeth will not obstruct the NFC antenna, and (ii) it is easier to manufacture than on the lingual surface.

[10]For example, in 2016 4.3 million [55], i.e. about 10% of adolescent population of the US from 2016, were treated with clear aligners.
[11]For the rest of this paper, we will use the term aligners to indicate both plastic aligners and retainers.

Fig. 4. Densor implementation. Left image—fabricated PCB before insertion into aligner: Ⓐ PCB antenna, Ⓑ STMicroelectronics ST25DV64K NFC tag [123], Ⓒ Seiko CPH3225A chip capacitor bank [112], Ⓓ Abracon AB1805 RTC [2], ⒺSTMicroelectronics LIS2DW12 accelerometer [121] , Ⓕ STMicroelectronics STM32L021F4 MCU [120], Ⓖ Vishay VEMD1060X01 photodiode [130], Ⓗ programming port (which is cut off before embedding in a dental aligner). Right image—example of a fully assembled Densor, i.e. fitted into a dental aligner.

6 Densor Implementation

With the Densor architecture presented, we proceed with the detailed description of its implementation. We start with the hardware (Section 6.1), followed by the software implementation (Section 6.2), and the integration of electronics with a dental aligner (Section 6.3).

6.1 Densor Hardware

6.1.1 NFC Interface. To implement the NFC interface, we use the STMicroelectronics ST25DV64K tag [123] for its energy harvesting capability and large on-chip NVM of 64 kbit.

6.1.2 Voltage Control. We chose the Fairchild Semiconductor MM3Z3V6C Zener diode [46] as an over-voltage protection device. An Nexperia 1PS76SB40 Schottky diode [92] was used to prevent current backfeed. Our circuit is kept simple to reduce the footprint and power consumption, as compared to an integrated voltage regulation circuit.

6.1.3 Energy Storage. The harvested energy from the NFC interface is stored on two parallel Seiko CPX3225A capacitors [112], 11 mF each, rated for a maximum voltage of 3.3 V. This is below the maximum allowed supply voltage of the MCU (3.6 V). As we will show in Section 7.1.4, the total capacitance determines the operation time of the Densor. Increasing the number of capacitors increases the lifetime of Densor, but simultaneously increases the charging time—reducing usability.

6.1.4 NFC Antenna. Commercially available NFC antennas we found could potentially cause discomfort [103], or be too fragile to withstand the jaw forces due to their ferrite core [79]. Hence, we designed a custom dual layer PCB 8 mm × 15 mm antenna using the STMicroelectronics inductance calculator [126]. We tested the antenna by connecting it to a Vector Network Analyzer (VNA) [115], and matched its impedance to an NFC reference antenna [122].

6.1.5 PMIC. For power control we use an Abracon AB1805 RTC [2] with integrated power switch, following the architecture presented in Section 5.1.4. We choose this PMIC as it has the lowest power consumption we could find, with the ability to switch the sensors off while inactive. The RTC is configured via Inter-Integrated Circuit (I2C) and is continuously powered by Densor's storage capacitors. All the sensors and the MCU on board of Densor are low-side switched (i.e the connection to ground is removed) by the RTC's power switch. This switching presents additional challenges as all possible paths between the switched components and ground have to be isolated. For example, the NFC chip is connected to the MCU via a pulled up I2C bus. The MCU can leak current to ground via this I2C path even when it is switched off. In order to isolate the NFC interface from the

power switched components, we use a TS3A44159 [127] switch for its small size and 1 nA supply current. The switch disconnects the I2C bus from the NFC chip when not in use, removing a potential leakage path. The RTC is clocked by its internal RC oscillator. However, if the user desires a higher clock frequency, they may use an external crystal. We note that as the crystal consumes extra energy, all results reported in Section 7 are measured using the RC oscillator clock source.

6.1.6 On-Board Sensors. We chose the STMicroelectronics LIS2DW12 accelerometer [121], as it has the ability to measure both temperature and acceleration with very low power consumption and a small physical form factor (2 mm × 2 mm). We chose the Vishay VEMD1060X01 photodiode [130] to measure light intensity. We use it in photoconductive mode to ensure linearity with incident light and fast response time. We placed the photodiode as close to the top edge of the PCB such that, once the Densor is placed inside the dental aligner, ambient light entering the mouth will not be permanently covered by the lips.

6.1.7 MCU. STMicroelectronics STM32L021F4 [120] was chosen for its small size (3 mm × 3 mm), low power consumption and versatile capabilities. The chosen MCU controls the I2C bus connected to the NFC tag, Power Management Integrated Circuit (PMIC) and accelerometer of Densor. The MCU also has the ability to perform analog measurements (like sampling the photodiode voltage) using the ADC.

6.1.8 PCB Fabrication. The Densor PCB was manufactured using flexible polyamide substrate with a thickness of 0.1 mm, which allows it to be curved into the shape of the jaw. An Electroless Nickel Immersion Gold (ENIG) surface finish was used, and the components were soldered on using a lead-free solder paste [88]. All components are placed on one side of the two-layer PCB, so that the Densor can sit flush against the teeth when enclosed. The PCB can be expanded to add more sensors (addressing Requirement ❼ from Section 4). An example of a fully assembled Densor is presented in Figure 4.

6.2 Densor Software

6.2.1 Densor Firmware. For the Densor firmware we implement the state diagram shown in Section 5.2.2 using STM32cubeMX [124]. As the MCU and all the on-board Densor sensors are all switched simultaneously, we have to introduce delays for them to start-up. The duration of these delays was found experimentally and were reduced to a minimum.

The analog measurements of the photo diode and temperature depend on the source voltage of the capacitors. This means that the falling source voltage of the draining capacitors affects the measurements. To overcome this, we find the linear relationship between the source voltage and measured values, and compensate all measurements to that of a corresponding stable supply voltage as explained in Appendix C.

6.2.2 Smartphone App. We developed a smartphone app based on the architecture in Section 5.2.1 that allows the user to configure the following Densor properties: (i) which sensors will be sampled (temperature, accelerometer or photodiode), (ii) which RTC clock source to use (crystal or RC), and (iii) sampling rate. The app can also display the Densor's charge level, synchronise the measurement to the wall clock, and read/write/clear memory. The app (seen on the screen of a smartphone shown in Figure 1) was developed in Java, based on ST25 NFC Tap App [125], and is compatible with Android 6.0 and higher.

6.3 PCB Integration with a Dental Aligner

First, a dental impression [131] of each test subject was taken using condensation silicone [35] placed on a dental impression tray. The hardened impression was later used to create a plaster model [24] of the subject's lower jaw teeth. Next, the plaster was placed inside an Erkoform-3d+ dental thermoforming unit [44]. Then, a dental thermoforming plate [45] was heated to 160 degrees Celcius by Erkoform-3d+, placed over the dental plaster and

vacuum sealed. After vacuum sealing, all redundant and sharp edges of the fabricated aligner were removed by the cut-off wheel. The remaining imperfections were removed with the same cut-off wheel, and finally disinfected. Based on previous studies using intraoral sensors, we find that epoxy resin is a suitable protective agent to seal the electronics from the oral cavity [57, Section 4.2].

With the aligner ready, two methods of attaching Densor to the transparent dental aligner were used.

Attachment using Silicone Layer: The Densor PCB is first attached to the center front side of the aligner with a silicone based dental putty [42]. Then a thin layer of bio-compatible epoxy resin [100] was applied to seal the electronics from moisture damage and for the safety of the user. The short curing time (6 min) and stickiness of the silicone allows us to fixate the PCB in the desired position. After this, the epoxy can be applied. The epoxy takes a few hours to harden and up to four days to cure completely. On the negative side, the lack of transparency of the silicone putty reduces the sensitivity of the light sensor.

Attachment Using Epoxy Resin: In this method, the Densor PCB was attached the same way as in the previous method, except for applying the dental putty first. This method is comparatively challenging as the PCB has to be held in place manually until the epoxy has sufficiently hardened. On the positive side, it does not obscure the light sensor.

We note that both integration processes depend on the regular dental aligner fabrication process. In other words, the Densor aligner fabrication does not require any specialized equipment that would not be already available to a dental technical.

7 Results

We proceed with the evaluation of Densor with a demonstration of intraoral sensing, as well as usage for sleep studies with accordance to the strategies described by Ledo et al. [74]. We divide the results into device benchmarks (Section 7.1), in vivo evaluation (Section 7.2) and the user acceptability study of intraoral sensors (Section 7.3).

7.1 Densor Benchmarks

7.1.1 Densor Physical Properties. Physical properties and code statistics of Densor are summarized in Table 1 (first column). The Densor PCB with assembled components (without aligner) weighs 0.26 g, and the fully assembled device (with aligner) weighs an average of 3.11 g. We conclude that Densor is the lightest of the actively powered battery-free platforms we have surveyed, and fits seamlessly into regular dental aligners.

7.1.2 Densor Software Characteristics. Densor's firmware code size was 9.73 kB, using 60.84% of the flash memory of the MCU [120, Page 1]. The Densor smartphone app code size was 10.55 MB, which is less than average for an Android app [21, Sec. 3] (data for 2019).

7.1.3 Densor Fabrication Cost. Fabrication of the Densor PCB costs (including the cost of all electronic components and shipment) approximately €22. The production cost of the aligners, including the cost of embedding of Densor into the aligner, was around €150. This price is typical for the country in which the Densor reported in this paper was fabricated in, and may differ with each country. Needless to say, the reported prices can decrease with higher production quantities due to economies of scale. For example, when producing 1000 units the cost of the assembled PCB will reduce to €6.35.

7.1.4 Densor Capacitors Charging Characterization. We proceed with the measurements of Densor's capacitor charging characteristics, i.e., charging duration and charging curve, using commercial smartphones. For the measurements we used three smartphones: iPhone 13, Google Pixel 3A and Google Pixel 6A. We used the Salea Pro 16 logic analyzer [108] to measure the voltage on the storage capacitors when charging via NFC using the smartphone, starting from fully discharged capacitors. The result is presented in Figure 5. We observe that

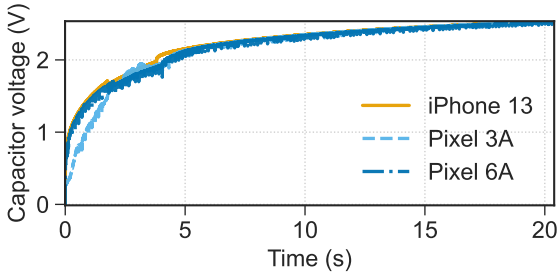

Fig. 5. Densor charging characterisation when charged with three different smartphones. Densor had two 11 mF on-board capacitors connected in parallel (refer to Figure 4). We conclude that charging time to 75% of full charging capacity of 3.3 V takes less than 20 s, irrespective of the smartphone used. The experiment was conducted with the assembled Densor PCB, as shown in Figure 4(left), lying flat on the back of each tested smartphone, close to the location of the NFC antenna with Densor PCB not moving for the entire duration of the measurement.

all three smartphones charge Densor following a similar charging pattern. It takes less than five seconds to charge Densor to 1.8 V, i.e., the minimum voltage required for Densor to operate. Around 20 s are needed to charge the Densor capacitor storage bank to ≈2.5 V, i.e. approximately 75% of the nominal 3.3 V capacity of the storage capacitors used. This result shows that Densor charging is fast and consistent with all tested smartphones. However, we note that no smartphone used in the experiments was able to charge the capacitors to their full 3.3 V value: the maximum voltage value we observed was 2.9 V. Charging requires precise alignment between the antennas of the smartphone and Densor. For all the in vivo results presented in this study, Densor was charged while outside the mouth using the feedback of charged capacitor voltage from the smartphone app. While it is also possible to charge Densor through the skin, i.e. cheeks, we did not evaluate this due to complexity of the experiment setup. In our subjective assessment based on example experiments, there is no major difference in charging behavior after the PCB is flexed and sealed into the aligner. However, as it is not possible to attach test probes after sealing, we were unable to measure voltage traces precisely as presented in Figure 5.

7.1.5 Densor Through-Skin Data Collection. We also tested whether it is possible to extract sensor data once the Densor is already in the mouth. We found that Densor can indeed interact with a smartphone (receive and transmit data) even when it is inside the mouth. We took three example measurements and found that it takes an average of 5.44 s (minimum and maximum of 4.66 s and 6.76 s, respectively) to read the full Densor memory of 64 kbit via NFC using the smartphone app and a Google Pixel 6A. This was measured with Densor worn in the mouth, and the smartphone touching the cheek at the place where the antenna is located.

7.1.6 Densor Energy Consumption. Using the Keithley 2450 source meter [65] connected to Densor storage capacitors (after Densor was charged and started regular operation) we characterized Densor current consumption. The result of this measurement is shown in Figure 6a. This current profile is composed of two states: peak current during operation I_r, and power off state I_o. The operation state is when the sensor is sensing and storing measurements, while the off state is when the sensors and the MCU is powered off. The values of I_r and I_o are reported in Table 2 in relation to the current consumption of other components of Densor. The length of the operation stage is 41 ms, measured with Salea Pro 16 logic analyzer [108]. The trace in Figure 6a is generated by combining the separately measured timing data and individual values of I_r and I_o.

We find that with measured I_r (which is 37 363 times higher than I_o assuming RTC is clocked by the RC oscillator, see Table 2), Densor can conduct approximately up to 500 operations starting from a full capacitor

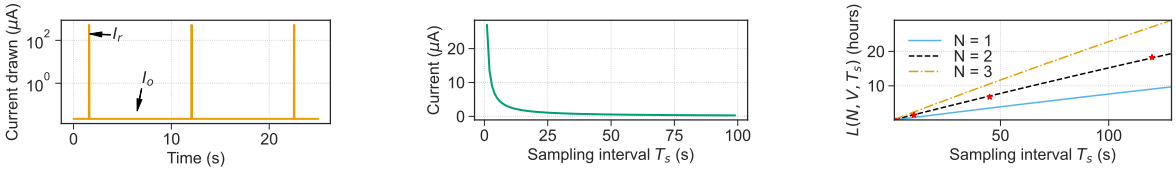

(a) Typical measured current drawn with ten second sampling interval.

(b) Modeled average current consumption as a function of T_s.

(c) Modeled (lines) and measured (*) lifetime with varying number of capacitors N.

Fig. 6. Characterization of current consumption and lifetime of the Densor, as presented in Section 7.1.6. Selected parameters for the center and right figure: $V = 3.3\,\text{V}$, $C = 11\,\text{mF}$.

charge of 3.3 V, regardless of the sensor sampling distribution of inter-sample time, since $I_\text{r} \gg I_\text{o}$. The maximum number of these operations was found experimentally by running Densor not embedded in dental aligner at 1 Hz sampling frequency, starting from a maximum capacitor storage of 3.3 V charged using an external power supply.

Densor Operation Lifetime Model. To estimate the lifetime of Densor as a function of number of capacitors N available to Densor, the voltage V to which they are charged and the sampling interval T_s, denoted as $L(N, V, T_\text{s})$, we model it as

$$L(N, V, T_\text{s}) = \frac{\text{Energy available}}{\text{Average power consumption}} = \frac{N\frac{1}{2}C\left(V^2 - V_\text{L}^2\right)}{V\left(\frac{I_\text{r}T_\text{r} + I_\text{o}(T_\text{s} - T_\text{r})}{T_\text{s}}\right)}, \tag{1}$$

where C is the total storage capacitance of Densor, $V_L = 1.8\,\text{V}$ is the minimum operating voltage of the Densor, T_r is the operation time of Densor (time spent on sampling all on-board sensors and storing the measurement on the on-device memory).

Briefly explaining Equation 1: in the numerator, to compensate for the energy that is unusable by Densor due to the fixed lower voltage threshold V_L, we subtract it from the current voltage V. The denominator represents the energy spent by the Densor per second, where the system runs for a fixed time T_r every sampling interval T_s.

Densor Operation Lifetime Model Numerical Examples. Figure 6b presents the total current draw ($I_\text{r} + I_\text{o}$) as a function of sampling interval T_s. This curve plots the denominator of Equation 1 excluding voltage V. Because $I_\text{r} \gg I_\text{o}$, the average current consumption of Densor reduces as the sampling interval increases.

Example Densor lifetime values estimated by our model are shown in Figure 6c, for $N = \{1, 2, 3\}$, together with the values from real measurements superimposed on the the lifetime function $L(N, V, T_\text{s})$. We see that with $T_\text{s} = 1$ sample per 100 s interval and $N = 3$ capacitors of 11 mF, Densor can sustain almost a whole day of operation with a single charge.

7.2 In Vivo Measurements with Densor

We now proceed with the functional evaluation of Densor. We show how Densor can classify different events such as open mouth, speaking or head position during sleep. We also report event classification accuracy.

7.2.1 *Measurement Setup and Data Collection.*

Human Subjects. Three authors of this work wore Densor attached to a custom-made retainer in various scenarios to collect labelled data. Use of Densor for experiments was approved by the Human Research Ethics Committee of the institution to which the authors of this work are associated.

Table 2. Densor current consumption.

Densor component	*Value*[†]
Schottky diode leakage [92, Fig. 2]	≈7.5 nA
NFC chip isolating switch [127, Sec. 6.5]	≈0.5 nA
MCU [120]	≈805 µA
Accelerometer [121, Table 4]	≈0.38 µA
RTC [2, Table 8]	14 nA (with RC oscillator); 55 nA (with crystal)
Total system: at idle time (I_o)[†]	22 nA (with RTC RC oscillator); 70 nA (with RTC crystal)
Total system: at operation (I_r)[†]	822 µA

[†] I_r and I_o are measured with Keithley 2450 source meter [65]; other values are taken from respective technical specifications of the producer.

Table 3. Set of tasks used for classification and training.

Task	Duration of task execution (seconds)
Head up during sleep	30
Head left during sleep	30
Head right during sleep	30
Wear Densor with mouth closed	15,[†]30
Wear Densor with mouth open	15,[†]30
Speaking with Densor inside the mouth	30
Drink water	5
Densor laying flat[‡]	60
Walk around with Densor in hand	60
Walk around with Densor in bag	60

[†] Used for Densor comparison with ear-based accelerometer
[‡] No exposure to varying light intensity is expected here

Controlled Experiments. All three users wore the Densor while performing activities listed in Table 3 that pertain to the following states that we aim to classify: (i) orthodontic compliance (to check whether an aligner was worn in the mouth), (ii) mouth opening state (open or close), (iii) speaking, (iv) fluid (water) intake, and (v) head position during sleep. First, the Densor was charged for approximately 1 min with a smartphone until the storage capacitor voltage reached 2.6 V as displayed on the app. Then, a computer script instructed the wearer of Densor to perform each task in a predefined (randomly shuffled) order—each for a specified duration. Because Densor is battery-free, the voltage level of the discharging capacitors might potentially affect the accuracy of the measurements from the sensors, and are compensated in software offline. Nonetheless, to remove any bias from this effect, the order of the activities were varied for each experiment run. The user remained in the same state for the entire duration of the task requested by the program. The data collected from the Densor (that is accelerometer, temperature and analog measurement of the light intensity using the photodiode) were all sampled at 1 Hz. At this sampling rate, Densor has a lifetime of approximately 8 min. An example of the raw data from all on-board sensors collected from these experiments, including the power budget, can be seen in Figure 7.

To synchronise the task labels from a Personal Computer (PC) to the collected measurements, Densor and the instructing script were started at the same time. The data points collected during transitions between activities were removed to account for any synchronisation inaccuracy. This is because it can take up to five seconds for the Densor to actually start after being enabled, and to account for reaction time of the user when activities change. A total of 57 experiments were performed by three users over multiple days with varying ambient conditions.

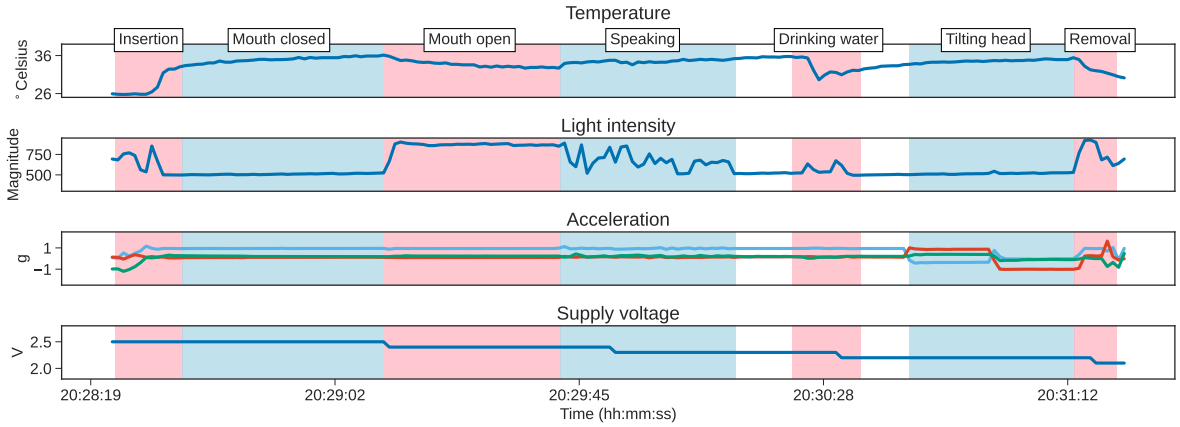

Fig. 7. Example data from an actual in vivo measurements collected at 1 Hz using Densor while performing various tasks. The measured temperature rises when Densor is inserted in the mouth, and dips when cold water is consumed. Light intensity rises when the mouth is open. Measured accelerations can determine the orientation of the jaw. The supply voltage is seen falling as the storage capacitors discharge during use.

Real-Life Experiments. In addition to the controlled experiments, one of the human subject participating in the experiments wore Densor during overnight sleep. The purpose of this data collection was to evaluate Densor in collecting sleep-related data. Nine datasets were collected from an overnight sleep between 19 March 2024 and 26 April 2024. For all sleep measurements Densor sampled data once every two minutes. At the beginning of each night measurement, right before placing Densor in the mouth, the user charged the Densor to at least 2.6 V using our developed Densor application installed on a smartphone (see Section 6.2.2).[12]

Reference System: In-Ear Accelerometer. To assess the effectiveness of Densor in performing mouth-related state classification, we built a simple hardware reference setup. That is, we developed a small rigid PCB with only a STMicroelectronics LIS2DW12 [121] (the same as the one used by Densor), which was then mounted inside a commodity, reusable music earplug from which the sound filter was removed and replaced with the PCB, see Figure 8. The ear-mounted accelerometer is connected to an external Arduino Leonardo [11] through an I2C bus, and samples the accelerometer output at 25 Hz with a 16 bit resolution. The data is saved to a file with a Unix time based timestamp. Later, the data is synchronised with that from the Densor based on the start time and activity list performed by the user.

7.2.2 Feature Extraction. We perform feature extraction to transform the raw sensor values into a set of relevant features, reducing dimensionality, noise, and complexity. To classify speaking from time series data, we calculate the variance of the light intensity signal. This is because when speaking, the measured light intensity changes rapidly as seen in Figure 7. For this controlled experiment, we assume the entire time series signal is purely speaking for 30 s (i.e without any transition in activity). To classify drinking, we extract the largest dip in the measured in the series of temperatures values, $f(x)$ as $\min_x f'(x)$. Finally, to make accelerations invariant to the orientation of the sensor while classifying movements, we extract the resultant acceleration as the magnitude of all three values from the accelerometer.

[12]During the experiments one of the following smartphones was used: Google Pixel 3A, Google Pixel 6A and Samsung Galaxy S8.

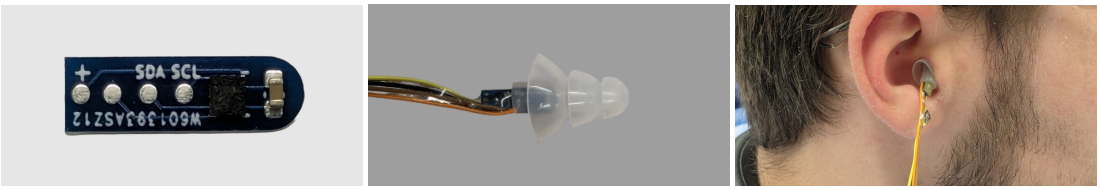

(a) Developed in-ear accelerometer board. PCB dimensions: 4 mm × 14 mm × 2 mm.

(b) Fabricated accelerometer board attached to the ear tip.

(c) Complete setup as worn by the subject.

Fig. 8. In-ear system for measuring acceleration values from an ear.

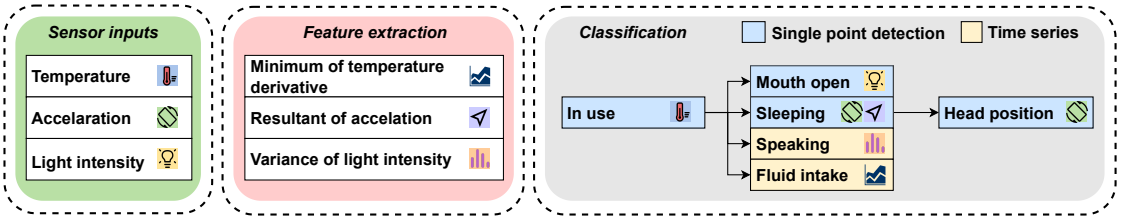

Fig. 9. Classified states by Densor mapped into sensor inputs and extracted signal features.

7.2.3 Classification. To classify the activities from these experiments, we used the labelled data collected, and trained a decision tree model offline using the `scikit-learn` software suite [99]. We choose a decision tree classifier for its low memory footprint and potential to be implemented on the on-board MCU of Densor, if necessary. The classification algorithm uses the multi-modal sensor inputs for step-by-step detection as seen in Figure 9. For instance, once we establish that the user is wearing Densor based on temperature readings, we can then use the light sensor to detect speaking as the next step. While some activities can be detected using a single data point, others such as speaking or drinking require features from time series data. As decision trees are prone to over-fitting the training data, we regularise the models by controlling the maximum depth of the tree and the minimum number of samples required in each leaf. 66% of all collected tasks were used for training the model, and the remaining 33% for evaluation.

7.2.4 State Classification. We proceed with the evaluation of the performance of state classification by Densor, refer again to all classified states which are listed in Figure 9.

Overall Classification Performance. Table 4 shows the results of all machine learning models. To ensure the predictions did not take place by chance, we verify that the p-value is < 0.01. As the fluid intake detection for participant P3 fails to meet this criteria, we exclude it from further analysis. Below we discuss some of the classification tasks in detail.

Orthodontic Compliance When embedded in an orthodontic aligner, Densor can help in collecting data on if the aligner is being worn. As seen in Figure 7, the temperature measured by Densor rises to human body temperature when Densor is worn by the user. With this insight, compliance can be determined by checking if the temperature is within range of oral temperature of the human body. As an illustration, a box plot of temperature recordings is seen in Figure 10a, alongside temperature measurements when Densor was not being worn. The

Table 4. Accuracy (in %) of four states classification (as described in Section 7.2.4) from decision tree classifications per user and fabrication method.

Participant	Densor attachment	Notes†	Measured range	Compliance	Mouth opening	Speaking	Fluid intake
P1	Silicone putty	**L**: Sealed **T**: Level	**L**: [511, 640] **T**: [32.8, 34.9]	100	79	–	–
P2	Epoxy resin	**L**: Exposed **T**: Protruding	**L**: [504, 1581] **T**: [27.7, 36.7]	100	91	100	100
P3	Epoxy resin	**L**: Exposed **T**: Level	**L**: [504, 2357] **T**: [32.0, 35.3]	100	92	80	70
All participants	–	–	–	100	90	91	100

Color scheme: $p < 0.01$; $p > 0.01$; insufficient data †Notes on Densor characteristics: *Sealed*: photodiode was partially covered by the silicone; *Exposed*: photodiode was covered with clear epoxy only; *Level*: temperature sensor was sitting flush against the aligner; *Protruding*: a gap between temperature sensor and aligner; **L**: light, **T**: Temperature.

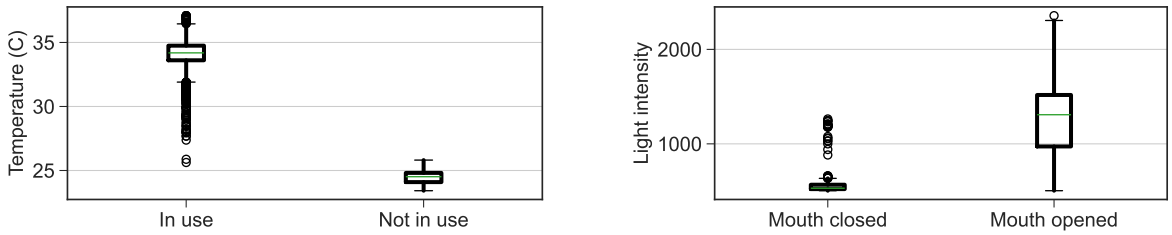

(a) In-mouth temperature depending on if Densor is in use.

(b) Light intensity depending on if user's mouth is open.

Fig. 10. Distribution of temperature and light intensity measured by Densor. Temperature data was collected from all three participants. Light intensity data was collected from participants wearing Densor attached using the epoxy resin only.

temperature measurements of Densor being worn include those of when the mouth was opened and closed, and during speaking and while drinking water. In our case, because the experiment was performed where the ambient temperature was a median of 24 °C, the detection accuracy was 100%. Thus, temperature measurement confirms actual usage of the device, providing feedback to the dental practitioner. We note that although this method is generally effective, it may fail if Densor is used in places where the ambient temperature is the same as human body temperature.

Mouth Opening State Detection. The Densor is able to detect if the user's mouth is open by measuring acceleration and light intensity from inside the mouth. To compare Densor's detection ability to an existing measurement benchmark, we use the reference setup described in Section 7.2.1 as a baseline. An example comparing a mouth closing event measured both from the ear and the mouth is seen in Figure 11. The example presented in Figure 11a and Figure 11b is of an exaggerated opening event, as the ear-mounted accelerometer is not sensitive enough to gentle movements. Additionally, the light intensity measured from inside the mouth using Densor can be seen in Figure 11c. Assuming the user is in a well lit environment, this is a more reliable source of mouth opening detection as it is independent of the opening or closing motion itself. Figure 12 shows the Receiver Operating Characteristic (ROC) curves for the decision trees trained on the signal outputs of both the ear-mounted accelerometer and the Densor. In Case 1 for the ear-mounted system, the in-ear accelerations

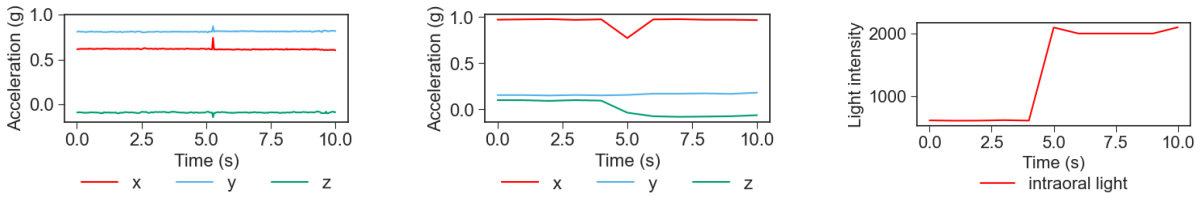

(a) Acceleration measured by in-ear accelerometer.

(b) Acceleration measured by Densor.

(c) Increase in intraoral light intensity measured by Densor.

Fig. 11. Example traces (simultaneously collected) from in-ear accelerometer and Densor during mouth opening. When the mouth is opened (at the five second mark) the in-ear accelerometer only records a change during the transition. The in-mouth accelerometer on Densor can recover the jaw orientation (pitch) directly—note the permanent change of the z direction once the mouth is open (center figure) compared to flat z direction for in-ear accelerometer (left figure). Additionally, Densor can measure intraoral light intensity to help the decision, which makes determining mouth opening state easier with Densor.

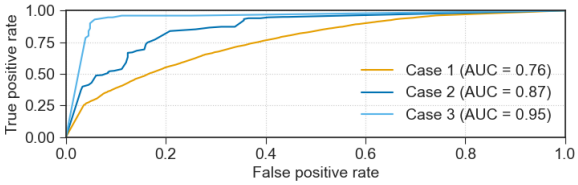

Fig. 12. ROC curve for detecting mouth opening state, i.e. open or close. Case 1: ear-mounted accelerometer, Case 2: Densor (accelerometer use only), Case 3: Densor (accelerometer and photodiode use). We conclude that Densor outperforms an ear-mounted system, while using a lower sampling frequency; AUC: area under the ROC curve.

are used as features. To make a fair comparison between the systems, two different models are trained on the Densor-generated data. Case 2 uses only Densor-generated accelerations and its resultant as features, to make it a comparable model to that of the the ear-mounted accelerometer. Case 3 includes all previous features and additionally light intensity, to showcase the capabilities of Densor. As can be seen, Densor outperforms the ear-mounted accelerometer significantly. From this we can conclude that Densor is better at detecting mouth states from a single measurement than a comparable system mounted inside the ear.

We note that, unfortunately, mouth opening state detection using photodiodes is limited to well-illuminated environments. This limitation can be overcome by using external infrared illumination which is invisible to the human eye. While the selected photodiode is also sensitive to infrared wavelengths, we do not explore this approach as it requires an external infrared light source, contrary to requirement ❺.

Fluid Intake. Densor measures a drop in temperature when the user consumes a cool liquid, such as tap water.[13] As we show in Table 4 classification accuracy depends on the Densor fabrication technique and physical characteristics of the fabricated Densor. On devices with a silicone-coated temperature sensor no temperature change was detected, presumably because the sensor was shielded from the flowing water. However, when attached to the aligner using only epoxy, Densor experienced temperature drops depending on the sensor's level of physical exposure to water. The temperature drop was more prominent when a gap was present in between the sensor and the teeth. Thus, we find a trade-off between accurate body temperature measurement, and sensitivity

[13]Note that only water is allowed to be consumed while wearing any aligner.

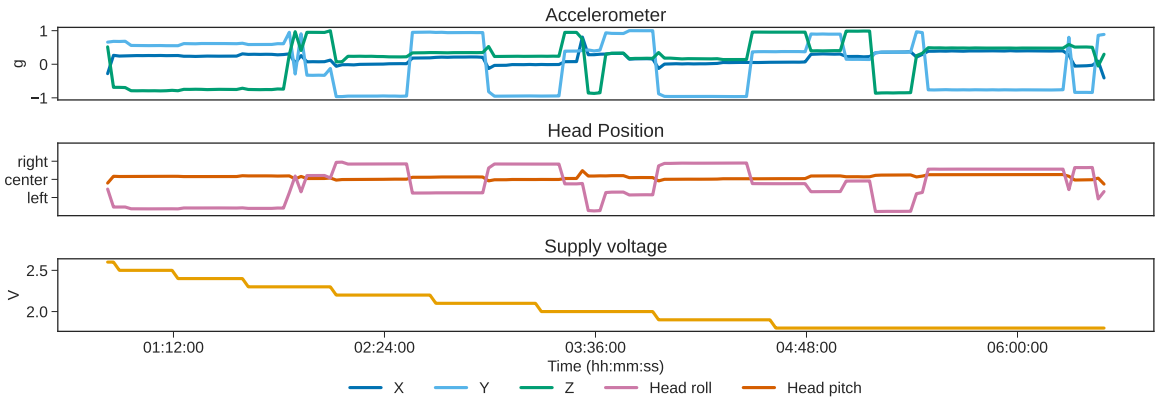

Fig. 13. Data from an actual in vivo measurements using Densor during sleep, with a measurement every 2 min over a period of 6 h 40 min. The head position (pitch and roll) are recovered from the acceleration measurements. Densor is able to sustain measurements for a full night's sleep on a single charge. Note: the step-wise function of supply voltage is due to a finite four bit precision to store voltage values.

to external factors like fluid intake. To overcome this limitation, multiple temperature sensors should be added in future revisions of Densor—one sensor for each purpose.

Sleep Studies. As most people with prescribed retainers wear them while asleep, it is an excellent signal source of the head position while sleeping. Using the accelerometer onboard Densor, we can recover the roll and pitch of the head, measured directly from the jaw. The head position measurements collected over one night's sleep can be seen in Figure 13. Since these measurements come directly from the sensor, we believe that machine learning is unnecessary. Still, to ensure the validity and accuracy of this measuring technique, we collected labelled data while laying in the supine and lateral positions (i.e facing upwards, and left and right side). We were able to identify that the user was lying down (sleeping position) with an accuracy of 100% and classify each position with a 99.8% accuracy. We note that as the position of the accelerometer varies with each user after attachment of the PCB to retainer—the roll and pitch need to be calibrated to zero when centered. This offset correction is done for each device specifically.

7.2.5 Endurance. We find that Densor sustained its functionality during the entire duration of the data collection—requiring no repairs, and no new fabrications. It performed reliably for the entire duration of all experiments spanning 48 days, even after multiple uses for overnight sleep monitoring.

7.2.6 Subjective Assessment of Wearing Comfort. Two out of three users wore Densor while asleep and found it comfortable, similar to wearing retainers. One participant used orthodontic wax to smooth sharp points for safety. Both users were able to wear the device while asleep without any difficulties, allowing its use in sleep studies and other long-duration applications.

7.3 Acceptability of Multimodal Intraoral Sensors

Each body area sensor will experience a different level of acceptability by the general population. Intraoral sensors are easily removable, eliminating the fear of surgery associated with implantable sensors [110, Figure 14a]. Yet, they are still located inside the human body. Widespread adoption of intraoral sensors depends not only on them being less invasive than implantable sensors, but also on their acceptability and the potential benefit

Table 5. Acceptability study demographics.

Parameter	Values
Sample size	116
Age [years] (mean, standard deviation σ)	28.8, 11.1
Gender (female, male, other)	47%, 52%, 1%
Education (BSc, MSc or professional degree, other)	68%, 25% ,7%
Background (dentistry, CS,[1] EE,[1] other)	66%, 9%, 7%, 18%
Active student (BSc, MSc, or PhD)	77%
Used dental aligners/retainers	59%
Heard of intraoral sensors	22%

[1] CS: Computer Science, EE: Electrical Engineering.

of wearing them. Some general studies on the perception of implantable medical technologies exist [110], but lack focus on oral cavity sensors. Studies of intraoral device acceptability exist [28], however, pertaining to a specific form factor (CR1220 coin cell battery size edible object). We are not aware of any study regarding generic intraoral sensors. Addressing this void, we performed the following experiment.

7.3.1 Methodology. An online survey was performed using Qualtrix XM [104] from the population sample chosen to represent individuals with sufficient technical knowledge in the fields of interest. The sample was selected out of convenience from the master-level courses for dentistry and engineering students (including computer science and biomedical engineering) from two different higher education institutions. Additionally, general dentists were approached during a study session of the local dentists' association.

The study was submitted for review to the medical ethical review commission of one of the centers involved in this study and was exempted from extensive ethical review. The protocol was registered a priori [106].

A desirable sample size of 100 was calculated a priori, assuming a default large source population of 1 000 000, an error of 10%, a confidence interval of 95%, a significance level of $p = 0.05$, and an expected proportion of 0.5, using OpenEpi [40]. The questionnaire used in this study was made in English and was pre-tested: eight staff members from the two institutions involved in the study were asked to respond to the questionnaire and give their opinion on each of the questions in open text fields. The researchers used the comments given by the participants to adapt the survey instrument and make a final version. The instrument had two types of questions, general questions to which all participants responded and specific questions to which participants with special backgrounds, (i.e., dentistry or students in any engineering field) responded.

At each of the survey sessions, first a presentation was given to potential respondents in which the desirable features of the device (e.g., wireless communications) and the potential health-related outcomes (e.g., jaw movements to detect tooth grinding or temperature to detect fever) were explained. Hereafter, a QR code was displayed for participants to start the questionnaire. The respondents were instructed to respond from the perspective of an end user. Participation was completely voluntary. The final structure of the survey, including the presentation, is available at [106].

7.3.2 Data Analysis. Demographic data was analysed descriptively. The survey answers were analyzed regarding the proposed hypothesis for each question, i.e., that the majority of individuals agreed or strongly agreed with the statement of the posed question. One proportion Z-tests were used to assess statistical significance of the survey proportions against 0.5. The script utilised for the analysis, along with the survey data, are available at [1].

7.3.3 Results. Demographic information of the participants is summarized in Table 5 and the results are presented in Figure 14. We conclude that the majority of the participants chose either "Agree" or "Strongly agree" for most

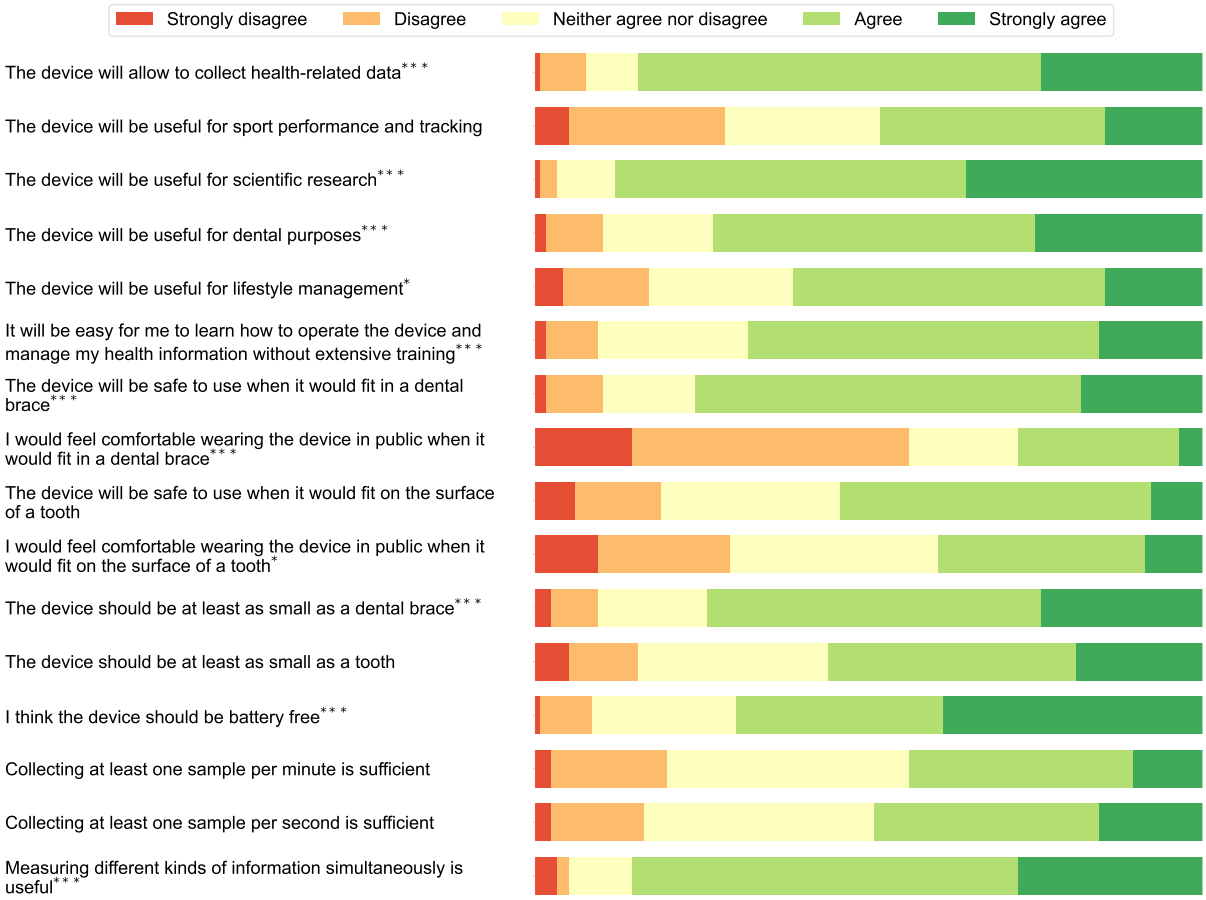

Fig. 14. Distribution of answers for each question stated in the acceptability study of intraoral sensors. Statistical tests performed based on the proportion of participants who chose "Agree" or "Strongly agree" on each question, against a default of 0.5. Symbols *, ** and *** denote $p < 0.05$, $p < 0.01$, and $p < 0.001$, respectively.

questions. The statements lacking a majority agreement were about the comfort of wearing the device in public. Regarding the specific questions for individuals in dentistry (see [1]), the majority of individuals agreed or strongly agreed with the usefulness of an intraoral sensor for tracking jaw movements, position of the tongue, and air passing through the mouth. For other uses, only a minority of individuals agreed. Other items in this section of the survey, such as whether intraoral sensing should be more common, or whether the participants had thought about intraoral sensing before, had low levels of agreement.

Discussion. We remark that, as noted in [28, Sec. 7], social acceptability is dependent on "context, individual, preferences, and culture", so the acceptability study we performed should be extended considering these factors.

8 Discussion

Densor requires further development and improvements. Here we discuss the most important ones.

Miniaturization. We desire that Densor is smaller than a tooth in its final form, and is invisible to others. Even if visible, it can be integrated with teeth jewelry [22, 87].

Towards continuous operation. Due to limited energy storage, Densor is unable to operate for a long period with high sampling rates, and therefore cannot record all intraoral events. However, sustaining continuous operation on an intermittently-powered device is an open research problem [75, 81]. Densor is yet another example of a battery-free device, and may contribute to understanding challenges associated with the battery-free devices [4].

Use of active transmission. Many prior intraoral sensing platforms used active wireless transmitters (often Bluetooth Low Energy (BLE)) to transmit live data from the intraoral sensor to the outside of the user's body. While we believe that live transmission is mostly unnecessary, it is appealing to equip Densor with a BLE transmitter from an engineering perspective. However, this is particularly challenging given the limited energy available.

Advancements in sensing. In this work we include three sensing modalities. The mouth offers the unique ability to measure many signals like tongue position, breathing, macro-nutrients and other bio-markers in saliva which can also be explored in future studies. The sensors enabling such measurements may require a power budget greater than that available with this battery-free design.

9 Conclusions

This paper presented Densor: a novel battery-free sensing platform for autonomous prolonged measurements of multiple signals originating from the human mouth. Densor is lightweight and easy to embed in regular dental aligners. Beyond the seamless detection of head position during sleep, Densor allows for a more accurate classification of jaw state compared to an in-ear accelerometer: all this done using fewer samples and on a battery-free power budget. An accompanying large-scale user study hints at potential wide scale acceptability of intraoral sensors for various applications, including healthcare.

Acknowledgments

We thank Tofik Babayev from TofDent, The Hague, The Netherlands, for help in fabricating all versions of the Densor. We also thank Giuseppe Deininger and Jakub Patałuch for contribution to the development of Densor at the initial states of the development. We also thank Lennart Klaver for first attempts in designing intraoral sensor hardware, Jasper de Winkel for system design consulting and Izabela Grudzińska for dentistry consulting and for the inspiration of this project. The study was partly funded by the ORANGE-FORCE project co-funded by the PPP allowance made available by Health Holland, Top Sector Life Sciences and Health.

References

[1] TU Delft Sustainable Systems Lab. 2024. Densor Source Code Repository: Hardware and Software Artifacts. https://github.com/TUDSSL/Densor. Last accessed: Oct. 9, 2024.

[2] Abracon Corp. 2014. AB18X5 Real-Time Clock. https://abracon.com/Precisiontiming/AB18X5-RTC.pdf. Last accessed: Feb. 16, 2024.

[3] Aesyra SA. 2023. AesyBite Active. https://www.aesyra.com. Last accessed: Mar. 4, 2024.

[4] Saad Ahmed, Bashima Islam, Kasım Sinan Yıldırım, Marco Zimmerling, Przemysław Pawełczak, Muhammad Hamad Alizai, Brandon Lucia, Luca Mottola, Jacob Sorber, and Josiah Hester. 2024. The Internet of Batteryless Things. *Commun. ACM* 67, 3 (2024), 64–73. https://doi.org/10.1145/3624718.

[5] Sayma Akther, Nazir Saleheen, Mithun Saha, Vivek Shetty, and Santosh Kumar. 2021. mTeeth: Identifying Brushing Teeth Surfaces Using Wrist-Worn Inertial Sensors. *ACM Interact. Mob. Wearable Ubiquitous Technol.* 5, 2 (2021), 53:1–53:24. https://doi.org/10.1145/3463494.

[6] Takashi Amesaka, Hiroki Watanabe, and Masanori Sugimoto. 2019. Facial Expression Recognition Using Ear Canal Transfer Function. In *Proc. ISWC* (Sept. 9–13). ACM, London, United Kingdom. https://doi.org/10.1145/3341163.3347747.

[7] Toshiyuki Ando, Yuki Kubo, Buntarou Shizuki, and Shin Takahashi. 2017. CanalSense: Face-Related Movement Recognition System based on Sensing Air Pressure in Ear Canals. In *Proc. UIST* (Oct. 22–25). ACM, Québec City, Canada, 679–689. https://doi.org/10.1145/3126594.3126649.

[8] Takahiro Arakawa, Yusuke Kuroki, Hiroki Nitta, Prem Chouhan, Koji Toma, Shin ichi Sawada, Shuhei Takeuchi, Toshiaki Sekita, Kazunari Akiyoshi, Shunsuke Minakuchi, and Kohji Mitsubayashi. 2016. Mouthguard Biosensor with Telemetry System for Monitoring of Saliva Glucose: A Novel Cavitas Sensor. *Biosensors and Bioelectronics* 84, 10 (2016), 106–111. https://doi.org/10.1016/j.bios.2015.12.01.

[9] Takahiro Arakawa, Keisuke Tomoto, Hiroki Nitta, Koji Toma, Shuhei Takeuchi, Toshiaki Sekita, Shunsuke Minakuchi, and Kohji Mitsubayashi. 2020. A Wearable Cellulose Acetate-Coated Mouthguard Biosensor for In Vivo Salivary Glucose Measurement. *Analytical Chemistry* 92, 18 (2020), 12201–12207. https://doi.org/10.1021/acs.analchem.0c01201.

[10] Takahiro Arakawa, Keisuke Tomoto, Hiroki Nitta, Koji Toma, Shuhei Takeuchi, Toshiaki Sekita, Shunsuke Minakuchi, and Kohji Mitsubayashi. 2020. A Wearable Cellulose Acetate-Coated Mouthguard Biosensor for In Vivo Salivary Glucose Measurement. *Analytical Chemistry* 92, 18 (2020), 12201–12207. https://doi.org/10.1021/acs.analchem.0c01201.

[11] Arduino S.r.l. 2024. Arduino Leonardo. https://docs.arduino.cc/hardware/leonardo. Last accessed: Apr. 29, 2024.

[12] H. Ceren Ates, Peter Q. Nguyen, Laura Gonzalez-Macia, Eden Morales-Narváez, Firat Güder, James J. Collins, and Can Dincer. 2022. End-to-End Design of Wearable Sensors. *Nature Review Materials* 7 (2022), 887–907. https://doi.org/10.1038/s41578-022-00460-x.

[13] Augmental Technologies Inc. 2023. MouthPad: A Tongue-Driven Interface. https://www.augmental.tech. Last accessed: Mar. 4, 2024.

[14] Amay J. Bandodkar and Joseph Wang. 2014. Non-Invasive Wearable Electrochemical Sensors: a Review. *Trends in Biotechnology* 32, 7 (2014), 363–371. https://doi.org/10.1016/j.tibtech.2014.04.005.

[15] Muath Bani-Hania and M. Amin Karamia. 2016. Energy Harvesting from Mastication Forces via a Smart Tooth. In *Proc. Sensors and Smart Structures Technologies for Civil, Mechanical, and Aerospace Systems* (March 21–24). SPIE, Las Vegas, NV, USA. https://doi.org/10.1117/12.2219390.

[16] Adam Bartsch, Sergey Samorezov, Edward Benzel, Vincent Miele, and Daniel Brett. 2014. Validation of an "Intelligent Mouthguard" Single Event Head Impact Dosimeter. *Stapp Car Crash Journal* 58, 11 (2014), 1–27. https://doi.org/10.4271/2014-22-0001.

[17] Eiko Bäumker, Luca Conrad, Laura Maria Comella, and Peter Woias. 2021. A Fully Featured Thermal Energy Harvesting Tracker for Wildlife. *Energies* 14, 16363 (2021). https://doi.org/10.3390/en14196363.

[18] Abdelkareem Bedri, David Byrd, Peter Presti, Himanshu Sahni, Zehua Gue, and Thad Starner. 2015. Stick It In Your Ear: Building an In-Ear Jaw Movement Sensor. In *Proc. Ubicomp/ISWC Adjunct* (Sept. 7–11). ACM, Osaka, Japan. https://doi.org/10.1145/2800835.2807933.

[19] Abdelkareem Bedri, Diana Li, Rushil Khurana, Kunal Bhuwalka, and Mayank Goel. 2020. FitByte Automatic Diet Monitoring in Unconstrained Situations Using Multimodal Sensing on Eyeglasses. In *Proc. CHI* (April 23–30). IEEE, Honolulu, HI, USA. https://doi.org/10.1145/3313831.3376869.

[20] Abdelkareem Bedri, Richard Li, Malcolm Haynes, Raj Prateek Kosaraju, Ishaan Grover, Temiloluwa Prioleau, Min Yan Beh, Mayank Goel, Thad Starner, and Gregory Abowd. 2017. EarBit: Using Wearable Sensors to Detect Eating Episodes in Unconstrained Environments. *ACM Interact. Mob. Wearable Ubiquitous Technol.* 1, 3 (2017), 37:1–37:20. https://doi.org/10.1145/3130902.

[21] Ashish Bijlani, Umakishore Ramachandran, and Roy Campbell. 2021. Where did my 256 GB go? A Measurement Analysis of Storage Consumption on Smart Mobile Devices. *ACM Meas. Anal. Comput. Syst.* 5, 2 (2021), 28:1–28:28. https://doi.org/10.1145/3460095.

[22] Siân Boyle. 2204. From £35 Crystals to £30,000 Diamonds: the Jaw-Dropping Rise of Tooth Jewellery. https://www.theguardian.com/fashion/2024/mar/05/from-35-crystals-to-30000-diamonds-the-jaw-dropping-rise-of-tooth-jewellery. Last accessed: Mar. 5, 2024.

[23] Braebon Medical Corp. 2013. DentiTrac. https://www.bnctechnologies.com/dentitrac.php. Last accessed: Mar. 4, 2024.

[24] Bredent GmbH & Co. KG. 2015. Highest Quality Plasters for Challenging Tasks. https://bredent-group.com/wp-content/uploads/2020/06/gipse-von-hoechster-Qualitaet_000727GB-20150601.pdf. Last accessed: Feb. 25, 2024.

[25] BruXane GmbH. 2020. BruXane Personal Aligner. https://bruxane.com/bruxane-personal. Last accessed: Mar. 4, 2024.

[26] byteSense. 2023. AI-Powered Smart Night Guard. https://www.bytesense.ai. Last accessed: Mar. 4, 2024.

[27] Yetong Cao, Huijie Chen, Fan Li, and Yu Wang. 2021. CanalScan: Tongue-Jaw Movement Recognition via Ear Canal Deformation Sensing. In *Proc. INFOCOM* (May 10–13). IEEE, Vancouver, BC, Canada. https://doi.org/10.1109/infocom42981.2021.9488852.

[28] Pablo Gallego Cascón, Denys J.C. Matthies, Sachith Muthukumarana, and Suranga Nanayakkara. 2019. ChewIt. An Intraoral Interface for Discreet Interactions. In *Proc. CHI* (May 4–9). ACM, Glasgow, Scotland, UK, 326:1–326:16. https://doi.org/10.1145/3290605.3300556.

[29] Nicholas J. Cecchi, August G. Domel, Yuzhe Liu, Eli Rice, Rong Lu, Xianghao Zhan, Zhou Zhou, Samuel J. Raymond, Sohrab Sami, Heer Singh, India Rangel, Landon P. Watson, Svein Kleiven, Michael Zeineh, David B. Camarillo, and Gerald Grant. 2021. Identifying Factors Associated with Head Impact Kinematics and Brain Strain in High School American Football via Instrumented Mouthguards. *Annals of Biomedical Engineering* 49, 10 (2021), 2814–2826. https://doi.org/10.1007/s10439-021-02853-5.

[30] Lam A. Cheah, James M. Gilbert, Jose A. Gonzalez, Jie Bai1, Stephen R. Ell, Phil D. Green, and Roger K. Moore. 2016. Towards an Intraoral-based Silent Speech Restoration System for Post-Laryngectomy Voice Replacement. In *Proc. Biomedical Engineering Systems and Technologies* (Feb. 21–23). Springer, Rome, Italy, 22–38. https://doi.org/10.1007/978-3-319-54717-6.

[31] Kaixin Chen, Lei Wang, Yongzhi Huang, Lu Wang, and Kaishun Wu. 2023. LiT: Fine-grained Toothbrushing Monitoring with Commercial LED Toothbrush. In *Proc. MobiCom* (Oct. 2–6). ACM, Madrid, Spain. https://doi.org/10.1145/3570361.3613287.

[32] Zipeng Cheng, Penghai Li, Jianying Teng, Yuan Wang, Shuli Deng, Bo Zhao, and Yuxuan Luo. 2023. A Dual-Layer Orthogonal-Layout Thin-Film Force Sensor for Digital Orthodontic Functional Appliances. *IEEE Sensors J.* 23, 15 (2023), 17524–17530. https:

//doi.org/10.1109/jsen.2023.3275943.
[33] Keum San Chun, Sarnab Bhattacharya, Caroline Dolbear, Jordon Kashanchi, and Edison Thomaz. 2020. Intraoral Temperature and Inertial Sensing in Automated Dietary Assessment: A Feasibility Study. In *Proc. ISWC* (Nov. 1–6). ACM, Virtual Event, Mexico, 27–31. https://doi.org/10.1145/3410531.3414309.
[34] Cleveland Clinic. 2022. Is It Safe to Sleep With Headphones or Earbuds? https://health.clevelandclinic.org/sleeping-with-headphones. Last accessed: Mar. 1, 2024.
[35] COLTENE Holding AG. 2024. Speedex Putty Condensation Silicone. https://products.coltene.com/EN/US/products/prosthetics/c-silicones/speedex/speedex-putty. Last accessed: Mar. 10, 2024.
[36] CUI Devices. 2022. Series: CP07-M, Description: Peltier Module. =https://www.cuidevices.com/product/resource/cp07-m.pdf. Last accessed: Mar. 3, 2024.
[37] Leonardo de Almeida e Bueno, Man Ting Kwong, and Jeroen H. M. Bergmann. 2023. Performance of Oral Cavity Sensors: A Systematic Review. *Sensors* 23, 588 (2023). https://doi.org/10.3390/s23020588.
[38] Jasper de Winkel, Carlo Delle Donne, Kasım Sinan Yıldırım, Przemysław Pawełczak, and Josiah Hester. 2020. Reliable Timekeeping for Intermittent Computing. In *Proc. ASPLOS*. ACM, Lausanne, Switzerland, 53–67. https://doi.org/10.1145/3373376.3378464.
[39] Jasper de Winkel, Haozhe Tang, and Przemysław Pawełczak. 2022. Intermittently-powered Bluetooth that Works. In *Proc. MobiSys* (Jun. 25–Jul. 1). ACM, Portland, OR, USA. https://doi.org/10.1145/3498361.3538934.
[40] Andrew G. Dean and Kevin M. Sullivan. 2004. Open Source Epidemiologic Statistics for Public Health (Version 3.01). https://www.openepi.com. Last accessed: Feb. 28, 2024.
[41] Aidin Delnavaz and Jérémie Voix. 2014. Flexible Piezoelectric Energy Harvesting from Jaw Movements. *Smart Materials and Structures* 23 (2014), 105020:1–105020:8. https://doi.org/10.1088/0964-1726/23/10/105020.
[42] DMG Chemisch-Pharmazeutische Fabrik GmbH. 2024. Silagum-Comfort. https://www.dmg-dental.com/en/solutions/permanent-prosthetics/underfilling-material/silagum-comfort. Last accessed: Mar. 10, 2024.
[43] August G. Domel, Samuel J. Raymond, Chiara Giordano, Yuzhe Liu, Seyed Abdolmajid Yousefsani, Michael Fanton, Nicholas J. Cecchi, Olga Vovk, Ileana Pirozzi, Ali Kight, Brett Avery, Athanasia Boumis, Tyler Fetters, Simran Jandu, William M. Mehring, Sam Monga, Nicole Mouchawar, India Rangel, Eli Rice, Pritha Roy, Sohrab Sami, Heer Singh, Lyndia Wu, Calvin Kuo, Michael Zeineh, Gerald Grant, and David B. Camarillo. 2021. A New Open-Access Platform for Measuring and Sharing mTBI Data. *Scientific Reports* 11, 7501 (2021). https://doi.org/10.1038/s41598-021-87085-2.
[44] Erkodent Erich Kopp GmbH. 2024. Erkoform-3d+ Thermoforming Unit. https://www.erkodent.de/en/product/?id=188600. Last accessed: Mar. 11, 2024.
[45] Erkodent Erich Kopp GmbH. 2024. Thermoforming Plate. https://www.erkodent.de/en/product/?id=521210. Last accessed: Mar. 10, 2024.
[46] Fairchild Semiconductor Corp. 2010. MM3Z2V4C–MM3Z75VC Zener Diodes. https://www.farnell.com/datasheets/2552645.pdf. Last accessed: Feb. 19, 2024.
[47] Mauro Farella, C. Loke, Sylvia Sander, A. Songini, M. Allen, L. Mei, and Richard D. Cannon. 2016. Simultaneous Wireless Assessment of Intra-Oral pH and Temperature. *Journal of Dentistry* 51 (2016), 49–55. https://doi.org/10.1016/j.jdent.2016.05.012.
[48] Yosuke Fukushima, Yoshie Sano, Yuta Isozaki, Mao Endo, Taketo Tomoda, Tomohisa Kitamura, Tsuyoshi Sato, Yoshito Kamijo, Yoshiyuki Haga, and Tetsuya Yoda. 2019. A Pilot Clinical Evaluation of Oral Mucosal Dryness in Dehydrated Patients Using a Moisture-Checking Device. *Clinical and Experimental Dental Research* 5, 2 (2019), 116–120. https://doi.org/10.1002/cre2.145.
[49] Lee F. Gabler, Nathan Z. Dau, Gwansik Park, Alex Miles, Kristy B. Arbogast, and Jeff R. Crandall. 2021. Development of a Low-Power Instrumented Mouthpiece for Directly Measuring Head Acceleration in American Football. *Annals of Biomedical Engineering* 49, 10 (2021), 2760–2776. https://doi.org/10.1007/s10439-021-02826-8.
[50] Lee F. Gabler, Samuel H. Huddleston, Nathan Z. Dau, David J. Lessley, Kristy B. Arbogast, Xavier Thompson, Jacob E. Resch, and Jeff R. Crandall. 2020. On-Field Performance of an Instrumented Mouthguard for Detecting Head Impacts in American Football. *Annals of Biomedical Engineering* 48, 11 (2020), 2599–2612. https://doi.org/10.1007/s10439-020-02654-2.
[51] Kai Geissdoerfer and Marco Zimmerling. 2021. Bootstrapping Battery-free Wireless Networks: Efficient Neighbor Discovery and Synchronization in the Face of Intermittency. In *Proc. NSDI*. USENIX, Virtual Event, 439–455. https://www.usenix.org/system/files/nsdi21-geissdoerfer.pdf.
[52] Martin Brandl Julius Grabner, Karlheinz Kellner, Franz Seifert, Johann Nicolics, Sabina Grabner, and Gerald Grabner. 2009. A Low-Cost Wireless Sensor System and Its Application in Dental Retainers. *IEEE Sensors J.* 9, 3 (2009), 255–262. https://doi.org/10.1109/jsen.2008.2012205.
[53] Hans Graf and Hans Rudolf Mühlemann. 1966. Telemetry of Plaque pH from Interdental Area. *Helvetica Odontologica Acta* 10, 2 (1966), 94–101. https://pubmed.ncbi.nlm.nih.gov/5957240/.
[54] Hans Graf and Hans Rudolf Mühlemann. 1969. Oral Telemetry of Fluoride Ion Activity. *Archives of Oral Biology* 14, 3 (1969), 259–263. https://doi.org/10.1016/0003-9969(69)90228-3.

[55] Jill Werman Harris. 2019. No More Brace Face? Teens Increasingly Use Clear Aligners. https://www.nytimes.com/2019/01/08/well/family/no-more-brace-face-teens-increasingly-use-clear-aligners.html. Last accessed: Mar. 10, 2024.

[56] Yoon Heenam, Hwang Suhwan, Jung Dawoon, Choi Sangho, Joo Kwangmin, Choi Jaewon, Lee Yujin, Jeong Do-Un, and Park Kwangsuk. 2015. Estimation of Sleep Posture Using a Patch-type Accelerometer Based Device. In *Proc. International Conference of the IEEE Engineering in Medicine and Biology Society (EMBC)* (Aug. 25–29). IEEE, Milan, Italy, 4942–4945. https://doi.org/10.1109/EMBC.2015.7319500.

[57] Zhizhang Hu, Amirmohammad Radmehr, Yue Zhang, Shijia Pan, and Phuc Nguyen. 2024. IOTeeth: Intra-Oral Teeth Sensing System for Dental Occlusal Diseases Recognition. *ACM Interact. Mob. Wearable Ubiquitous Technol.* 8, 1 (2024), 7:1–7:29. https://doi.org/10.1145/3643516.

[58] Hua Huang and Shan Lin. 2020. MET: A Magneto-Inductive Sensing Based Electric Toothbrushing Monitoring System. In *Proc. MobiCom* (Sept. 21–25). ACM, London, UK. https://doi.org/10.1145/3372224.3380896.

[59] Kenta Ichikawa and Wataru Hijikata. 2022. Energy Harvesting from Biting Force with Thin Sheet Harvester Based on Electret and Dielectric Elastomer. *Nano Energy* 99 (2022). https://doi.org/10.1016/j.nanoen.2022.107357.

[60] International Organization for Standardization/International Electrotechnical Commission. 2018. ISO/IEC 14443-1:2018; Cards and Security Devices for Personal Identification; Contactless Proximity Objects; Part 1: Physical Characteristics. https://www.iso.org/standard/73596.html. Last accessed: Feb. 14, 2024.

[61] International Organization for Standardization/International Electrotechnical Commission. 2018. ISO/IEC 15693-1:2018; Cards and Security Devices for Personal Identification; Contactless Vicinity Objects; Part 1: Physical Characteristics. https://www.iso.org/standard/70837.html. Last accessed: Mar. 9, 2024.

[62] Bing Jiang, Jeonghee Kim, and Hangue Park. 2022. Palatal Electrotactile Display Outperforms Visual Display in Tongue Motor Learning. *IEEE Trans. Neural Syst. Rehabil. Eng.* 30 (2022), 529–539. https://doi.org/10.1109/tnsre.2022.3156398.

[63] Fahim Kawsar, Chulhong Min, Akhil Mathur, Alessandro Montanari, Utku Günay Acer, and Marc Van den Broeck. 2018. Demo Abstract: eSense - Open Earable Platform for Human Sensing. In *Proc. SenSys* (Nov. 4–7). ACM, Shenzhen, China, 371–372. https://doi.org/10.1145/3274783.3275188.

[64] Giannis Kazdaridis, Nikos Sidiropoulos, Ioannis Zografopoulos, Polychronis Symeonidis, and Thanasis Korakis. 2020. Nano-things: Pushing Sleep Current Consumption to the Limits in IoT Platforms. In *Proc. IoT*. ACM, Malmö, Sweden, 1–8. https://doi.org/10.1145/3410992.3410998.

[65] Keithley Instruments, LLC. 2021. 2450 SourceMeter Source Measurement Unit Instrument. https://download.tek.com/datasheet/1KW-60904-2_2450_Datasheet_072021.pdf. Last accessed: Sep. 11, 2021.

[66] Eun Joong Kim, Ji Ho Choi, Kang Woo Kim, Tae Hoon Kim, Sang Hag Lee, Heung Man Lee, Chol Shin, Ki Yeol Lee, and Seung Hoon Lee. 2011. The impacts of Open-Mouth Breathing on Upper Airway Space in Obstructive Sleep Apnea: 3-D MDCT Analysis. *European Archives of Oto-Rhino-Laryngology* 268 (2011), 533–539. https://doi.org/10.1007/s00405-010-1397-6.

[67] Jayoung Kim, Somayeh Imani, William R. de Araujo, Julian Warchall, Gabriela Valdès-Ramèrez, Thiago R.L.C. Paixão, Patrick P. Mercier, and Joseph Wang. 2015. Wearable Salivary Uric Acid Mouthguard Biosensor with Integrated Wireless Electronics. *Biosensors and Bioelectronics* 74 (2015), 1061–1068. https://doi.org/10.1016/j.bios.2015.07.039.

[68] Jayoung Kim, Somayeh Imani, William R. de Araujo, Julian Warchall, Gabriela Valdés-Ramírez, Thiago R.L.C. Paixão, Patrick P. Mercier, and Joseph Wang. 2015. Wearable Salivary Uric Acid Mouthguard Biosensor with Integrated Wireless Electronics. *Biosensors and Bioelectronics* 74 (2015), 1061–1068. https://doi.org/10.1016/j.bios.2015.07.039.

[69] Jayoung Kim, Gabriela Valdès-Ramìrez, Amay J. Bandodkar, Wenzhao Jia, Alexandra G. Martinez, Julian Ramìrez, Patrick Mercier, and Joseph Wang. 2014. Non-Invasive Mouthguard Biosensor for Continuous Salivary Monitoring of Metabolites. *Analyst* 7, 139 (2014), 1632–1636. https://doi.org/10.1039/c3an02359a.

[70] Jeffrey J. Kim, Gery R. Stafford, Carlos Beauchamp, and Shin Ae Kim. 2020. Development of a Dental Implantable Temperature Sensor for Real-Time Diagnosis of Infectious Disease. *Sensors* 20 (2020), 3953:1–3953:18. https://doi.org/doi:10.3390/s20143953.

[71] Stacey Kirshenblatt, Hui Chen, Marijke Dieltjens, Benjamin Pliska, and Fernanda R. Almeida. 2018. Accuracy of Thermosensitive Microsensors Intended to Monitor Patient Use of Removable Oral Appliances. *Journal of the Canadian Dental Association* 84, i2 (2018), 1–9. https://jcda.ca/sites/default/files/i2_0.pdf.

[72] Mayank Kohli, Li-Fang Hsu, Chin-Chung Chen, Chung-Chen Jane Yao, and Tien-Kan Chung. 2023. Wearable Wireless Magnetic-Reluctance-Based Pressure Sensing Module for Intraoral Pressure Monitoring. *IEEE Trans. Magn.* 59, 11 (2023). https://doi.org/10.1109/tmag.2023.3290768.

[73] Fanpeng Kong, Maysam Ghovanloo, and Gregory D. Durgin. 2020. An Adaptive Impedance Matching Transmitter for a Wireless Intraoral Tongue-Controlled Assistive Technology. *IEEE Trans. Circuits Syst. II, Exp. Briefs* 67, 2 (2020), 240–244. https://doi.org/10.1109/tcsii.2019.2913623.

[74] David Ledo, Steven Houben, Jo Vermeulen, Nicolai Marquardt, Lora Oehlberg, and Saul Greenberg. 2018. Evaluation Strategies for HCI Toolkit Research. In *Proc. CHI* (April 21–26). ACM, Montreal, QC, Canada, 36:1–36:17. https://doi.org/10.1145/3173574.3173610.

[75] Seulki Lee, Bashima Islam, Yubo Luo, and Shahriar Nirjon. 2019. Intermittent Learning: On-Device Machine Learning on Intermittently Powered System. *ACM Interact. Mob. Wearable Ubiquitous Technol.* 3, 4 (Dec. 2019), 141:1–141:30. https://doi.org/10.1145/3369837.

[76] Yongkuk Lee, Connor Howe, Saswat Mishra, Dong Sup Lee, Musa Mahmood, Matthew Piper, Youngbin Kim, Katie Tieu, Hun-Soo Byun, James P. Coffey, Mahdis Shayan, Youngjae Chun, Richard M. Costanzo, and Woon-Hong Yeo. 2018. Wireless, Intraoral Hybrid Electronics for Real-Time Quantification of Sodium Intake Toward Hypertension Management. *PNAS* 115, 21 (2018), 5377–5382. https://doi.org/10.1073/pnas.1719573115.

[77] Yuanfang Li, Hao Tanga, Ying Liu, Yancong Qiaoa, Hongqi Xia, and Jianhua Zhou. 2022. Oral Wearable Sensors: Health Management Based on the Oral Cavity. *Biosensors and Bioelectronics: X* 10, 100135 (2022). https://doi.org/10.1016/j.biosx.2022.100135.

[78] Yuzhe Liu, August G. Domel, Seyed Abdolmajid Yousefsani1 Jovana Kondic, Gerald Grant, Michael Zeineh, and David B. Camarillo. 2020. Validation and Comparison of Instrumented Mouthguards for Measuring Head Kinematics and Assessing Brain Deformation in Football Impacts. *Annals of Biomedical Engineering* 48, 11 (2020), 2580–2598. https://doi.org/10.1007/s10439-020-02629-3.

[79] Logomotion, s.r.o. 2022. Micro Coil NFC Antennas. https://logomotion.eu/micro-coil-nfc-antenna/. Last accessed: Feb. 12, 2024.

[80] Lura Health. 2023. Tooth-Mounted Salivary Health Monitor. https://www.lurahealth.com. Last accessed: Mar. 4, 2024.

[81] Amjad Y. Majid, Patrick Schilder, and Koen Langendoen. 2020. Continuous Sensing on Intermittent Power. In *Proc. IPSN*. IEEE, Sydney, NSW, Australia, 181–192. https://doi.org/10.1109/IPSN48710.2020.00-36.

[82] Manu S. Mannoor, Hu Tao, Jefferson D. Clayton, Amartya Sengupta, David L. Kaplan, Rajesh R. Naik, Naveen Verma, Fiorenzo G. Omenetto, and Michael C. McAlpine. 2012. Graphene-based Wireless Bacteria Detection on Tooth Enamel. *Nature Communications* 3, 763 (2012), 1–8. https://doi.org/10.1038/ncomms1767.

[83] MATRIX Industries. 2019. Nanopower Energy Harvesting Synchronous Boost Converter with Microwatt Cold-Start, Input Impedance Matching and Regulated Output. https://www.mouser.com/datasheet/2/1000/MATRIX_Industries_09062019_MCRY12-125Q-42DI-1634489.pdf. Last accessed: Mar. 3, 2024.

[84] Hidekazu Matsumoto, Keisuke Tomoto, Gentaro Kawase, Kenta Iitani, Koji Toma, Takahiro Arakawa, Kohji Mitsubayashi, , and Keiji Moriyama. 2023. Real-Time Continuous Monitoring of Oral Soft Tissue Pressure with a Wireless Mouthguard Device for Assessing Tongue Thrusting Habits. *Sensors* 23 (2023), 5027:1–5027–12. https://doi.org/10.3390/s23115027.

[85] Hidekazu Matsumoto, Keisuke Tomoto, Gentaro Kawase, Kenta Iitani, Koji Toma, Takahiro Arakawa, Kohji Mitsubayashi, and Keiji Moriyama. 2023. Real-Time Continuous Monitoring of Oral Soft Tissue Pressure with a Wireless Mouthguard Device for Assessing Tongue Thrusting Habits. *Sensors* 23, 11 (2023). https://doi.org/10.3390/s23115027.

[86] MC Technology GmbH. 2024. Theramon Microsensor. https://www.thera-mon.com. Last accessed: Mar. 2, 2024.

[87] Melz Grillz. 2024. Custom Dental Grillz. https://www.melzgrillz.co/custom-grillz. Last accessed: Mar. 5, 2024.

[88] MG Chemicals. 2024. 4900P–SAC305 Solder Paste–No-Clean. https://mgchemicals.com/products/soldering-supplies/solder-paste/sac305-solder/. Last accessed: Mar. 11, 2024.

[89] Chochanon Moonla, Don Hui Lee, Dinesh Rokay, Natcha Rasitanon, Goma Kathayat, Won-Yong Lee, Jayoung Kim, and Itthipon Jeerapan. 2022. Review—Lab-in-a-Mouth and Advanced Point-of-Care Sensing Systems: Detecting Bioinformation from the Oral Cavity and Saliva. *ECS Sensors Plus* 1, 2 (2022). https://doi.org/10.1149/2754-2726/ac7533.

[90] Florian 'Floyd' Mueller, Pedro Lopes, Paul Strohmeier, Wendy Ju Caitlyn Seim, Martin Weigel, Suranga Nanayakkara, Marianna Obrist, Zhuying Li, Joseph Delfa, Jun Nishida, Elizabeth M. Gerber, Dag Svanaes, Jonathan Grudin, Stefan Greuter, Kai Kunze, Thomas Erickson, Steven Greenspan, Masahiko Inami, Joe Marshall, Harald Reiterer, Katrin Wolf, Jochen Meyer, Thecla Schiphorst, Dakuo Wang, and Pattie Maes. 2020. Next Steps in Human-Computer Integration. In *Proc. CHI* (April 25–30). ACM, Honolulu, HI, USA. https://doi.org/10.1145/3313831.3376242.

[91] Tanya Nandkeoliar, Ashish Kumar, Sachidananda Chungkham Singh, and Sinam Subhaschandra. 2023. Estimation of Vestibular Depth: An Observational Cross-Sectional Study. *Journal of Indian Society of Periodontology* 27, 3 (2023), 320–327. https://doi.org/10.4103/jisp.jisp_293_22.

[92] Nexperia B.V. 2015. BAS40 Series; 1PSxxSB4x Series General-Purpose Schottky diodes. https://docs.rs-online.com/6796/0900766b81270f45.pdf. Last accessed: Feb. 19, 2024.

[93] NFC Forum. 2024. Technical Overview Website. https://nfc-forum.org/learn/nfc-technology. Last accessed: Mar. 9, 2024.

[94] Emer O'Hare, John A. Cogan, Frank Dillon, Madeleine Lowery, and Eoin D. O'Cearbhaill. 2022. An Intraoral Non-Occlusal MEMS Sensor for Bruxism Detection. *IEEE Sensors J.* 22, 1 (2022), 153–161. https://doi.org/10.1109/jsen.2021.3128246.

[95] Shijia Pan, Dong Yoon Lee, Jun Ho Lee, and Phuc Nguyen. 2021. TeethVib: Monitoring Teeth Functional Occlusion Through Retainer Vibration Sensing. In *Proc. Conference on Connected Health: Applications, Systems and Engineering Technologies* (Dec. 16–18). IEEE/ACM, Washington D.C., USA, 92–96. .

[96] Nicoletta Panunzio, Gianluca Ligresti, Margherita Losardo, Donato Masi, Alessio Mostaccio, Francesca Nanni, Giulia Tartaglia, and Gaetano Marrocco. 2021. Cyber-Tooth Antennified Dental Implant for RFID Wireless Temperature Monitoring. In *Proc. RFID-TA* (Oct. 6–8). IEEE, Delhi, India, 211–214. https://doi.org/10.1109/rfid-ta53372.2021.9617316.

[97] Hangue Park and Maysam Ghovanloo. 2014. Wireless Communication of Intraoral Devices and its Optimal Frequency Selection. *IEEE Trans. Microw. Theory Tech.* 62, 12 (2014), 3205–3215. https://doi.org/10.1109/tmtt.2014.2365804.

[98] Hangue Park, Mehdi Kiani, Hyung-Min Lee, Jeonghee Kim, Jacob Block, Benoit Gosselin, and Maysam Ghovanloo. 2012. A Wireless Magnetoresistive Sensing System for an Intraoral Tongue-Computer Interface. *IEEE Trans. Biomed. Circuits Syst.* 6, 6 (2012), 571–585. https://doi.org/10.1109/TBCAS.2012.2227962.

[99] Fabian Pedregosa, Gaël Varoquaux, Alexandre Gramfort, Vincent Michel, Bertrand Thirion, Olivier Grisel, Mathieu Blondel, Peter Prettenhofer, Ron Weiss, Vincent Dubourg, Jake Vanderplas, Alexandre Passos, David Cournapeau, Matthieu Brucher, Matthieu Perrot, and Édouard Duchesnay. 2011. Scikit-learn: Machine Learning in Python. *Journal of Machine Learning Research* 12, 85 (2011), 2825–2830. hhttps://jmlr.org/papers/v12/pedregosa11a.html.

[100] Polyestershoppen BV. 2024. Epoxy Resin. https://polyestershoppen.com/epoxy/voedselveilige-epoxy-419.html. Last accessed: Apr. 28, 2024.

[101] William R. Proffit, Henry W. Fields, Brent E. Larson, and David M. Sarver. 2019. *Contemporary Orthodontics (Sixth Edition).* Elsevier, Philadelphia, PA, USA. ISBN 978-0-323-54387-3.

[102] ProSomnus Sleep Technologies. 2019. ProSomnus Device for Treatment of Sleep Apnea and Snoring. https://prosomnus.com. Last accessed: Apr. 30, 2024.

[103] Pulse Electronics, Inc./Larsen Antennas. 2024. 13.56 MHz RFID/NFC SMD Antenna (Part number W3102). https://productfinder.pulseelectronics.com/part/w3102. Last accessed: Feb. 13, 2024.

[104] Qualtrix. 2024. XM Platform. https://www.qualtrics.com/uk/platform/. Last accessed: Feb. 28, 2024.

[105] Andrea M. Rich, Tanner M. Filben, Logan E. Miller, Brian T. Tomblin, Aaron R. Van Gorkom, Michael A. Hurst, Ryan T. Barnard, Dena S. Kohn, Jillian E. Urban, and Joel D. Stitzel. 2019. Development, Validation and Pilot Field Deployment of a Custom Mouthpiece for Head Impact Measurement. *Annals of Biomedical Engineering* 47, 10 (2019), 2109–2121. https://doi.org/10.1007/s10439-019-02313-1.

[106] Víctor Ignacio Madariaga Rivera, Przemysław Pawełczak, and Vivian Dsouza. 2024. 'Acceptability of Multimodal Intraoral Sensors' Study Pre-Registration. https://osf.io/n32d4. Last accessed: Oct. 9, 2024.

[107] Tobias Röddiger, Tobias King, Dylan Ray Roodt, Christopher Clarke, and Michael Beigl. 2022. OpenEarable: Open Hardware Earable Sensing Platform. In *Proc. UbiComp/ISWC'22 Adjunct* (Sept. 11–15). ACM, Cambridge, UK, 246–251. https://doi.org/10.1145/3544793.3563415.

[108] Saleae, Inc. 2021. Logic Pro 16 USB Logic Analyzer. http://downloads.saleae.com/specs/Logic+Pro+16+Product+Fact+Sheet.pdf. Last accessed: Aug. 19, 2021.

[109] G. Sannino, D. Sbardella, E. Cianca, M. Ruggieri, M. Coletta, and R. Prasad. 2016. Dental and Biological Aspects for the Design of an Integrated Wireless Warning System for Implant Supported Prostheses: A Possible Approach. *Wireless Personal Communications* 88 (2016), 85–96. https://doi.org/10.1007/s11277-016-3244-6.

[110] Anne Kathrin Schaar and Martina Ziefle. 2011. What Determines Public Perceptions of Implantable Medical Technology: Insights into Cognitive and Affective Factors. In *Proc. Information Quality in e-Health* (Nov. 25–26). Springer, Graz, Austria, 513–531. https://doi.org/10.1007/978-3-642-25364-5_36.

[111] Rickne C. Scheid and Gabriela Weiss. 2012. *Woelfel's Dental Anatomy (Eight Edition).* Lippincott, Williams and Wilkins, Philadelphia, PA, USA. ISBN 978-1-60831-746-2.

[112] Seiko Instruments. 2024. CPH3225A Chip Capacitor. https://www.sii.co.jp/en/me/datasheets/chip-capacitor/cph3225a/. Last accessed: Feb. 14, 2024.

[113] SelfSense Technologies. 2021. SmartSplint. https://selfsense.ie. Last accessed: Mar. 4, 2024.

[114] Zhenghan Shi, Yanli Lu, Shuying Shen, Yi Xu, Chang Shu, Yue Wu, Jingjiang Lv, Xin Li, Zupeng Yan, Zijian An, Chaobo Dai, Lingkai Su, Fenni Zhang, and Qingjun Liu. 2022. Wearable Battery-Free Theranostic Dental Patch for Wireless Intraoral Sensing and Drug Delivery. *npj Flexible Electronics* 6, 1 (2022). https://doi.org/10.1038/s41528-022-00185-5.

[115] Siglent Technologies. 2024. SVA1015X 1.5 GHz Spectrum and Vector Network Analyzer. https://www.siglent.eu/product/1137207/siglent-sva1015x-1-5ghz-spectrum-vector-network-analyzer. Last accessed: Feb. 14, 2024.

[116] Akbarian Sina, Delfi Ghazaleh, Zhu Kaiyin, Yadollahi Azadeh, and Taati Babak. 2019. Automated Non-Contact Detection of Head and Body Positions During Sleep. *IEEE Access* 7 (2019), 72826–72834. https://doi.org/10.1109/access.2019.2920025.

[117] Somnomed Ltd. 2021. SomnoDent Oral Devices. https://somnomed.com/en/patients/products/somnodent/. Last accessed: Apr. 30, 2024.

[118] STM32World Wiki. 2022. STM32 Internal Temperature and Voltage Reference. https://stm32world.com/wiki/STM32_internal_temperature_and_voltage_reference. Last accessed: Jul. 31, 2024.

[119] STMicroelectronics N.V. 2014. AN4509 Tilt Measurement Using a Low-G 3-Axis Accelerometer. https://www.st.com/resource/en/application_note/dm00119046-tilt-measurement-using-a-low-g-3-axis-accelerometer-stmicroelectronics.pdf. Last accessed: Feb. 26, 2024.

[120] STMicroelectronics N.V. 2017. Ultra-low-power Arm Cortex-M0+ MCU with 16-Kbytes of Flash Memory, 32 MHz CPU, AES. https://www.st.com/resource/en/datasheet/stm32l021f4.pdf. Last accessed: Feb. 16, 2024.

[121] STMicroelectronics N.V. 2019. LIS2DW12 3-axis MEMS Accelerometer, Ultra Low Power, Configurable Single/Double-Tap Recognition, Free-Fall, Wakeup, Portrait/Landscape, 6D/4D Orientation Detections. https://www.st.com/resource/en/datasheet/lis2dw12.pdf. Last

accessed: Feb. 16, 2024.
[122] STMicroelectronics N.V. 2022. 14 mm × 14 mm Double Layer Antenna Reference Board for the ST25DV64KC Dual Interface EEPROM. https://www.st.com/en/evaluation-tools/ant7-t-25dv64kc.html. Last accessed: Feb. 14, 2024.
[123] STMicroelectronics N.V. 2023. Dynamic NFC/RFID Tag IC with 64-Kbit EEPROM, and Fast Transfer Mode Capability. https://www.st.com/resource/en/datasheet/st25dv64k.pdf. Last accessed: Feb. 16, 2024.
[124] STMicroelectronics N.V. 2023. STM32Cube Initialization Code Generator. https://www.st.com/en/development-tools/stm32cubemx.html. Last accessed: Mar. 10, 2024.
[125] STMicroelectronics N.V. 2024. Application Executable of the NFC Tap Android app for ST25 product family—Version 3.9.0. https://www.st.com/en/embedded-software/stsw-st25001.html. Last accessed: Mar. 11, 2024.
[126] STMicroelectronics N.V. 2024. NFC Inductance (version 1.7.0 - 231117) Design Tool. https://eds.st.com/antenna/. Last accessed: Feb. 14, 2024.
[127] Texas Instruments. 2024. TS3A44159 Quad SPDT Analog Switch. https://www.ti.com/lit/ds/symlink/ts3a44159.pdf?ts=1708948686558. Last accessed: Feb. 26, 2024.
[128] Peter Tseng, Bradley Napier, Logan Garbarini, David L. Kaplan, and Fiorenzo G. Omenetto. 2018. Functional, RF-Trilayer Sensors for Tooth-Mounted, Wireless Monitoring of the Oral Cavity and Food Consumption. *Advanced Materials* 30 (2018), 1703257:1–1703257:7. https://doi.org/10.1002/adma.201703257.
[129] Hiroko Tsuda, Alan A. Lowe, Hui Chen, John A. Fleetham, Najib T. Ayas, and Fernanda R. Almeida. 2011. The Relationship Between Mouth Opening and Sleep Stage-Related Sleep Disordered Breathing. *Journal of Clinical Sleep Medicine* 7, 2 (2011), 181–186. https://doi.org/10.5664/jcsm.28107.
[130] Vishay Intertechnology, Inc. 2016. VEMD1060X01 Silicon PIN Photodiode. https://www.vishay.com/docs/84295/vemd1060x01.pdf. Last accessed: Feb. 16, 2024.
[131] Wikipedia Editors. 2023. Dental Impression. https://en.wikipedia.org/wiki/Dental_impression. Last accessed: Feb. 25, 2024.
[132] WIRED Staff. 2006. Lying Through Their Teeth. https://www.wired.com/2006/04/lying-through-their-teeth. Last accessed: Mar. 5, 2024.
[133] Fan Yang, Ashok Samraj Thangarajan, Sam Michiels, Wouter Joosen, and Danny Hughes. 2021. Morphy: Software Defined Charge Storage for the IoT. In *Proc. SenSys*. ACM, Coimbra, Portugal, 248–260. https://doi.org/10.1145/3485730.3485947.
[134] Vincent Yi-Fong Su, Kun-Ta Chou, Chun-Hsien Tseng, Chia-Yu Kuo, Kang-Cheng Su, Diahn-Warng Perng, Yuh-Min Chen, and Shi-Chuan Chang. 2023. Mouth Opening/Breathing is Common in Sleep Apnea and Linked to More Nocturnal Water Loss. *Biomedical Journal* 46, 3 (2023), 100536:1–100536:9. https://doi.org/10.1016/j.bj.2022.05.001.
[135] Takuma Yoshitani, Masa Ogata, and Koji Yatani. 2016. LumiO: A Plaque-Aware Toothbrush. In *Proc. UbiComp* (Sept. 12–16). ACM, Heidelberg, Germany, 605—-615. https://doi.org/10.1145/2971648.2971704.
[136] Shichao Yue, Yuzhe Yang, Hao Wang, Hariharan Rahul, and Dina Katabi. 2020. BodyCompass: Monitoring Sleep Posture with Wireless Signals. *Proc. ACM Interact. Mob. Wearable Ubiquitous Technol.* 4, 2 (2020). https://doi.org/10.1145/3397311.
[137] Yi Zhao, Joshua R. Smith, and Alanson Sample. 2015. NFC-WISP: A Sensing and Computationally Enhanced Near-Field RFID Platform. In *Proc. IEEE RFID* (April 15–17). IEEE, San Diego, CA, USA. https://doi.org/10.1109/rfid.2015.7113089.

A Methodological Transparency and Reproducibility Appendix

To aide the reproducibility of this work, the design and all data collected will be released at the time of publication via a public repository [1]. This includes the files for hardware design, firmware, source code for the smartphone app, data collected, machine learning implementation and a description on how to reproduce the results presented in this work.

B Thermal Energy Harvesting

We performed a set of experiments to evaluate the amount of thermal energy generated from drinking cold water. We used two CP076581 Thermoelectric Generator (TEG) [36] in series, along with the MCRY12-125Q-42DI harvester [83] enclosed in retainers on a dental cast in the center of the lower jaw, with cables extending out of the TEG to measure the harvested energy. We found the maximum amount of energy harvested (from temperature differential between water and the human body) to be 7 mJ when 200 mL of water was consumed at 5 °C.

C Compensation of Falling Source Voltage

In a controlled experiment, we found that the temperature measurement drops by 1.4 °C per volt as the supply voltage of Densor falls. This experiment was performed using an external power supply at a consistent temperature. As Densor operates between 1.8 V and 3.3 V, we assume the measurement at the center value,V_{center}, of 2.5 V to be correct. Thus, when measuring temperature, t_{m}, the Densor app calculates the compensated reading, t_{c}, as

$$t_{\text{c}} = t_{\text{m}} - V_{\text{drop}}(V_{\text{supply}} - V_{\text{center}}), \tag{2}$$

where V_{supply} is the measured supply voltage, and V_{drop} is 1.4 V. Similarly, the photodiode measurements also need to be compensated for the falling supply voltage V_{supply}. As the measurements, p_{m}, are proportional to source voltage at runtime, we calculate the compensated photodiode value, p_{c}, as

$$p_{\text{c}} = V_{\text{supply}}(p_{\text{m}}/2^{12}), \tag{3}$$

where p_{m} is normalised by its maximum value of 2^{12} .